Received 23 September 2021; revised 14 October 2021; accepted 14 October 2021. Date of publication 19 October 2021; date of current version 29 October 2021.

Digital Object Identifier 10.1109/OJAP.2021.3121102

Origami Antennas

STAVROS V. GEORGAKOPOULOS [1] (Senior Member, IEEE), CONSTANTINOS L. ZEKIOS [1] (Member, IEEE), ABDUL SATTAR-KADDOUR [1] (Member, IEEE), MUHAMMAD HAMZA [1] (Graduate Student Member, IEEE), AKASH BISWAS [1] (Graduate Student Member, IEEE), BROOKLYN CLARK [2], COLLIN YNCHAUSTI [2], LARRY L. HOWELL [2], SPENCER P. MAGLEBY [2], AND ROBERT J. LANG [3] (Member, IEEE)

[1] Department of Electrical and Computer Engineering, Florida International University, Miami, FL 33174, USA

[2] Department of Mechanical Engineering, Brigham Young University, Provo, UT 84602, USA

[3] Lang Origami, Altadena, CA 91001, USA

CORRESPONDING AUTHOR: C. L. ZEKIOS (e-mail: kzekios@fiu.edu)

This work was supported in part by the Air Force Office of Scientific Research under Grant FA9550-18-1-0191 and Grant FA9550-19-1-0290, and in part by the Utah NASA Space Grant Consortium.

ABSTRACT The field of foldable and physically reconfigurable antennas has recently attracted significant interest from diverse scientific communities, including researchers on antennas, material science, mechanical engineering and numerical modeling. Deployable, packable and multifunctional systems are very important for many applications, including satellite communications, UAVs, CubeSats as well as airborne and spaceborne communication systems. Foldable and physically reconfigurable antennas, particularly origami-based antennas, can provide new capabilities for the aforementioned applications. In this work, we present emerging research on foldable and physically reconfigurable antennas. Such antennas morph their shape to adapt and reconfigure their EM performance (e.g., frequency of operation, bandwidth, polarization, beamwidth, etc.). Also, origami antennas provide ultra-compact stowage, easy deployment, reduced weight, enhanced EM performance and multifunctional utility.

INDEX TERMS Antennas, electromagnetics, origami, reconfigurable.

I. INTRODUCTION

RECONFIGURABLE, tunable, multifunctional, deployable, and ultra-wideband (UWB) high-performance antenna systems are expected to play a significant role in next-generation communication, reconnaissance, sensing, energy harvesting systems for airborne, spaceborne and terrestrial applications. Towards this goal, in recent years, significant advances have been made in: 1) antenna miniaturization, 2) UWB antennas with as much as 10:1 bandwidth or larger, 3) antenna reconfiguration using micro-electro-mechanical systems (MEMS) and phase-change material (PCM) switches, 4) antenna design with the use of fractal geometries (e.g., [1]), 5) conductive textiles for flexible antennas, 6) conductive inks and flexible materials, and 7) smart materials for actuation and sensing. Recently, origami folding techniques have been used to develop origami-based antennas, thereby creating a new class of physically reconfigurable electromagnetic (EM) structures that are easily deployable, efficiently packable, and operationally multifunctional. Origami-based designs have the unique ability to morph (i.e., transform) 2-*D* manifolds (not necessarily flat) into a continuous range of 2-*D* or 3-*D* shapes with temporal control via deterministic mechanisms thereby pioneering the development of rigid foldable systems. Therefore, origami antenna technologies are expected to provide new capabilities to various systems, including small Unmanned Aircraft Systems (UAS), drones, airborne and spaceborne systems, small satellites (cubesats and nanosats), deployable reflectors, and expandable reconfigurable surfaces. For example, when origami antennas are launched into space, they can be folded and stowed in small compartments, and when they reach orbit, they deploy into large apertures to communicate with ground stations on earth (see Fig. 1). Also, origami technologies address

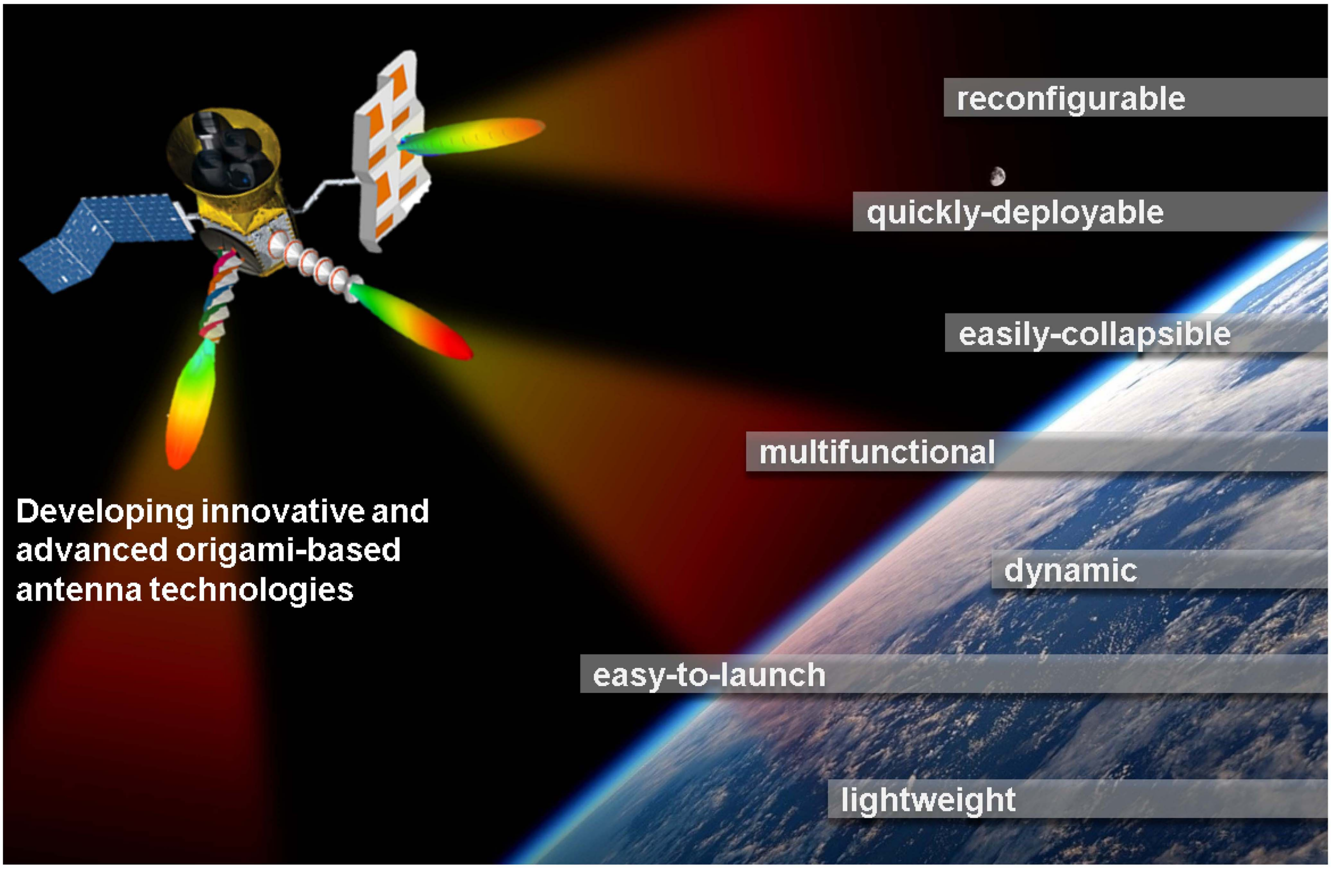

FIGURE 1. Origami antenna technologies will provide new capabilities to future communication systems.

important challenges of traditional tactical antennas that are heavy, bulky and static, by enabling the development of compact/collapsible, easy-to-deploy, lightweight and carry/wear reconfigurable antennas that increase the operational agility and mobility of operators in the field.

Section II provides a brief review of origami and identifies the mathematical challenges that are introduced when the mechanics of real-life systems are modeled. Section III reviews origami patterns used in mechanical engineering applications, with the main focus being on mechanical considerations of origami antennas. In Section IV a brief review on origami antennas is performed, while in Section V we present the evolution of our research on origami antennas. Section VI briefly presents our recently introduced computational toolset for the design and electromagnetic analysis of origami antennas. Section VII demonstrates the design process and analysis of a novel origami antenna, which is introduced here for the first time. Sections VIII and IX present a summary of the key advantages of origami antennas and identify important challenges that must be overcome to fully realize their potential.

II. REVIEW OF ORIGAMI

The practice of origami (interpreted broadly as "decorative or functional paper-folding" has a deep history in Japan (from which we get the name *origami*) and Europe [2] in various forms, e.g., napkin-folding [3], [4]. While the most well-known forms of origami, such as the iconic *tsuru* (crane) are primarily decorative, paper-folding with a functional purpose has long been a part of the practice, ranging from containers such as the Japanese *tato* [5], fan-folded codices of Mesoamerican culture [6], privacy-preserving European letter folds [7], and more.

The functional uses of origami (and folding in general) often relate to a goal of size reduction and shape transformation of a fundamentally sheet-like medium (not necessarily paper, as we will shortly see). This property of origami takes on particular significance when it comes to structures destined for space. Solar arrays, antennas, and optical components are all large and sheet-like in their deployed state, but must be reduced in size during launch to fit in the transport rocket, a need that can be summarized as "small for the journey, large at the destination." If the object is made of relatively stiff material (which is usually the case), then the deformations must be limited to localized regions, e.g., folds. For such objects and applications, folding patterns adapted from the world of origami can provide efficient, effective solutions for deployable structures and mechanisms.

One of the earliest space-borne origami structures was the JAXA Space Solar Flyer (SSF) [8], a test of a deployable solar array based on the now well-known Miura-Ori folding pattern [9] [see Fig. 2(a)]. (Although the SSF was arguably

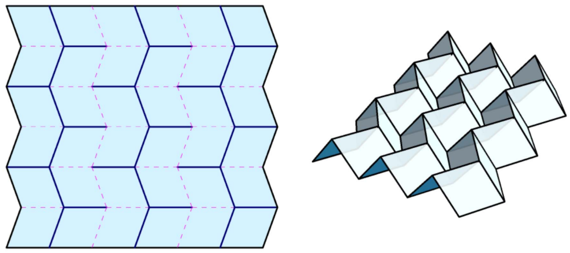

FIGURE 2. Crease pattern and folded form of Miura-Ori.

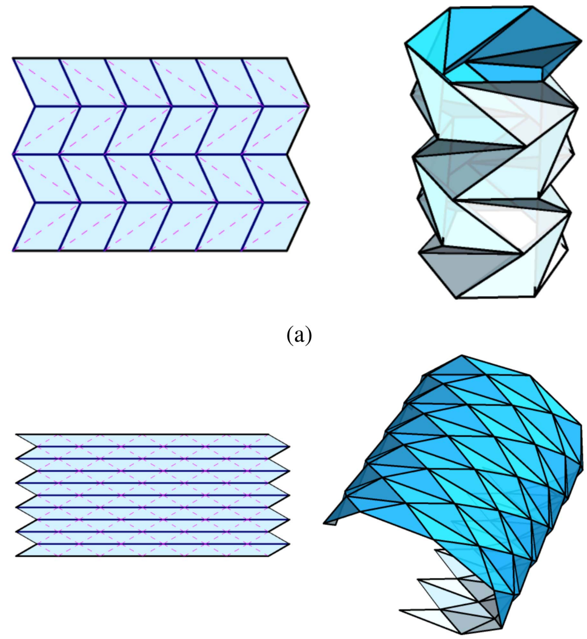

(a)

(b)

FIGURE 3. Crease pattern and folded form of: a) Kresling, and b) Yoshimura.

the first distinctively origami-based solar array, Z-folded solar arrays have been a mainstay of space solar configurations for decades [10].) Other space-based/origami-based optical structures include the Eyeglass [11], a diffractive optical lens developed in the early 2000s, and StarShade [12], [13], an occulter currently under development at NASA/JPL. The field of space-based/origami-based antennas is particularly rich; the introduction of the CubeSat architecture based on quantized multiples of 10 *cm* cubes created a particularly tight and quantitative bound on stowed size, leading to a number of innovative solutions [14]–[22].

The field of deployable structures and mechanisms includes families of mechanisms that go far beyond origami—see [23] for a general overview—and origami-like patterns include more than the traditional single-uncut-square paradigm of traditional origami. Origami-adapted and origami-inspired patterns [24], [25] can not only be non-square (as they usually are), but also non-developable (composed of surfaces with nonzero Gaussian curvature), pointwise non-developable (containing vertices whose total surrounding angle is greater or less than 2π), can contain holes, and/or can be non-manifold (e.g., containing 3 or more facets joined along a single fold). In broad terms, we can say a form is origami-like if it

- is composed of sheet-like regions, called *facets*;
- which are joined along linear compliant regions, called *folds*; folds meet each other or the boundary of the form at *vertices*;
- contains *interior vertices*, vertices that are not on the boundary of the form.[1]

One of the earliest patterns considered for space and which has seen ample application in the area of origami antennas is the *Miura-Ori* pattern (see Fig. 2) already mentioned. Although it was first described in a space/scientific context by Miura *et al.* [9], it has a much longer history; a 1959 patent by Hochfeld [26] shows a machine for pleating whose output is recognizably the Miura-Ori pattern. It may also be seen in the 1920s work of the Bauhaus group [27] in fact, it can be seen in illustrations from Giegher [3]. The basic doubly periodic Miura-Ori pattern can be characterized by three quantities: two side lengths and one angle of its build-block parallelogram. The concept, however, can be generalized to a variety of 3*D* shapes by selectively altering distances and angles within the pattern in one dimension, resulting in a *semi-generalized Miura-Ori* [28]. With careful control of the flat-foldability condition at vertices, two-dimensionally varying (nonperiodic) patterns may also be achieved [29].

Although a Miura-Ori can be trimmed to any shape in the deployed state, its stowed state and the symmetry of its motion is generally rectangular. A second broad family of patterns has a deployment motion that is generally cylindrical, and indeed, it takes the form generally of a triangulated cylinder. Two common varieties are the *Kresling* pattern [30] and *Yoshimura* pattern [31]; the former [see Fig. 3(a)] can be viewed as a helical version of the latter [see Fig. 3(b)]. In both cases, the 3*D* forms are long cylinders; the stowed form is a flattened version of the cylinder. Like the Miura-Ori, this family of patterns has deep antecedents; it can be seen, for example, in decorative cloth-folding going back centuries (including in the sleeve of the Mona Lisa [28]). With suitable choice of angles and dimensions, the Kresling pattern exhibits tunable multistable behavior as shown by Guest and Pellegrino [32]–[34]; by combining alternating helicity and/or cuts, a wide variety of deployment motions are possible [35], [36], many of which are adaptable for origami antenna applications.

A third family of patterns has a deployment pattern that combines rotary and radial deployment. Most commonly called the *Flasher* pattern (after a family of origami designs

1. This condition removes fan-folding/Z-folding from consideration as "origami-like," though they do contain folds. Many of the unusual properties (and challenges in design, simulation, and realization) of origami-like patterns come from the presence and properties of interior vertices, so we consider them essential elements to deserve the "origami-like" characterization.

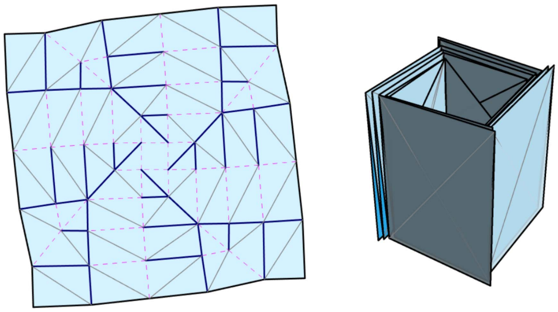

FIGURE 4. Crease pattern and folded form of planar flasher.

by Lang [37]), its deployed form takes the form of a circle, which collapses and wraps around a smaller cylindrical hub (see Fig. 4). Like the other patterns, versions existed outside the world of origami; a 1974 patent by Scheel [38] shows a wrapping device that uses the flasher pattern, and a mathematical analysis was carried out by Guest and Pellegrino [39]. A mathematical prescription for designing flashers with the layers spread-out to accommodate thickness was given by Zirbel *et al.*, [40]. While most initial work resulted in a flat circular disk in the deployed state, the concept (and analytical technique of Zirgel *et al.*) can and has been extended to result in non-developable surfaces in the deployed state, such as paraboloids [41], realized as parabolic reflectors for antennas. The Miura-Ori pattern can also be realized in a radially symmetric form [42], which offers the same radial/wrapping expansion and a cylindrical stowed state, but has multistable deployment. Yet another family of radial deployment patterns is based on the notion of *slip-wrapping* [43]–[45], which includes cuts and wrapping of flexible surfaces; this technique offers some of the highest deployed-to-stowed size ratios yet demonstrated.

When it comes to mathematically modeling origami, there is a rough hierarchy of approximation, with varying tradeoffs between simplicity of modeling and accuracy in capturing the physics and mechanics of the form:

- *Zero-Thickness Model:* The simplest modeling (which can still be surprisingly complex) is the planar-facet *zero-thickness model*, in which facets are treated as planar, folds are straight, and the full pattern can be treated as a polytope of linked vertices, edges and faces (corresponding, respectively, to vertices, folds, and facets in origami terminology). Within this approximation, there are two broad approaches: plate-based [46], in which the facets are treated as rigid bodies joined by revolute joints at folds, and truss-based [47], [48], in which the surface is triangulated and isometry preserved by length constraints on the edges.
- *Thickness:* A next step up is to accommodate thickness, which in most antenna applications, is non-negligible. The zero-thickness model can be used to approximate mechanisms with non-negligible thickness by treating the underlying structure as zero-thickness but embedding it within finite-thickness slabs; this approach can be used to preserve kinematic behavior [49]. However, the thickness can also disrupt the kinematics of real mechanisms, necessitating particular strategies in design to model and achieve kinematic motion in deployment. An overview of several approaches may be found in [50].
- *Curved Folding:* "Curved folding" can mean two different things: first, that the folds themselves are softly curved, rather than sharp; this can be addressed in modeling by an extension of the plate model, by incorporating cylindrical or conical plates (see, e.g., [51]). Second, the surfaces and folds themselves could be curved. The modeling of curved folds and their surrounding surfaces requires differential geometry; folding-specific references include [52]–[56].
- *Stretching and Bending:* Although most modeling assumes perfect isometry and (often) planar facets, real-world materials deform; even something as simple as the Miura-Ori exhibits deformation modes such as twisting and bending due to bending of the facets; other patterns exhibit compliance due to stretching or deformations that can be modeled by stretching. In these cases, truss-based models can be modified to incorporate strain energy associated with edge length changes and/or flexing along diagonals of polygonal facets, as well as strain energies associated with elastic and inelastic deformations of the folds themselves [57].

Based on these mathematical models, several computational tools have been developed to facilitate the design and modeling of origami structures for antenna applications.

- *Origamizer [58]:* A GUI-based program that can find a development (unfolding) of most triangulated surfaces.
- *Freeform Origami [59]:* Interactive manipulation of the vertices of a $3D$ form with real-time updating of the $2D$ development.
- *Ori-Revo [60]:* Generation of surfaces of rotation, including paraboloids and other surfaces suitable for antenna reflectors.
- *Tessellatica [61]:* A *Mathematica* package for the design and analysis of a wide variety of origami forms.
- *Origami Simulator [62]:* A fast Javascript simulator for folding a specified crease pattern into $3D$.
- *FOLD Format [63]:* A file format specification and suite of tools for importing, rendering, and translating folded state descriptions among other formats, providing interoperability between formats.

III. ORIGAMI IN ENGINEERING

Origami principles have been used to create products in a variety of applications. Some biomedical applications include stent grafts [64], drug delivery [65], and micro-grippers [66]. Origami has also been used in a variety of space applications, such as solar arrays [67], inflatable booms [68], and sunshields [69]. Consumer products benefited by the inspiration of origami include a reconfigurable light [70], a foldable pocket knife [71], and a collapsible

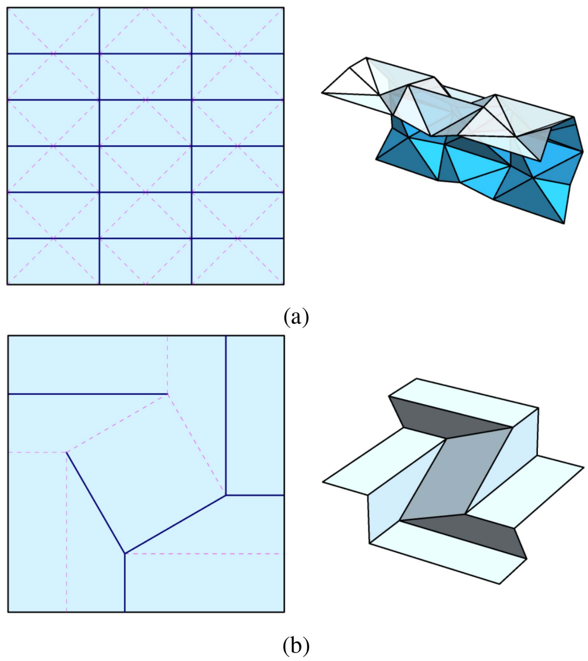

FIGURE 5. Crease pattern and folded form of: a) Waterbomb array, and b) Square twist.

stroller [72]. Mechatronic applications of origami include a compactly-stowing quadrotor [73], as well as various robots [74], [75].

Some of the most used origami patterns in mechanical engineering applications as discussed earlier are the Miura-Ori [76]–[84], the Yoshimura [84]–[87], the waterbomb [84], [88]–[91], twists [92]–[95], and flasher patterns [11], [67], [96]–[99].

The Miura-Ori (see Fig. 2) is a pattern consisting of a series of degree-4 vertices and has a single degree of freedom. This pattern is flat-foldable, rigid-foldable (panels do not deform during deployment motion) and overconstrained [100]. It has a negative Poisson's ratio, meaning it expands in one direction while expanding in the other direction when deployed [101]. It has been used in various engineering applications, particularly for space applications.

The Yoshimura pattern [see Fig. 3(b)] is a tessellation formed of adjacent, bisected, rhombi. All folds on the edges of the rhombi are mountain (or valley) with the bisection folds being valleys (or mountains). When compressed, the pattern folds in on itself. This pattern results from a buckling of a cylinder when it is compressed axially [102]. Unlike the Miura-Ori, this pattern does not have a single degree of freedom, due to its degree-6 vertices which have three degrees of freedom [94]. The Yoshimura pattern has been used in pneumatic actuators [103], energy absorption [104], and in the development of a barrel vault [105].

The waterbomb pattern [see Fig. 5(a)] is a degree-6 or degree-8 vertex with each crease alternating mountain and valley. The degree-6 vertex is 3 degrees of freedom mechanism [106]. The waterbomb pattern has been studied as a test-bed for programmable materials [107], for application in worm robots [108], and as a deformable robot wheel [109].

Twists are patterns composed of a single central polygonal panel with other panels formed by parallel lines extending from each vertex of the central polygon [see Fig. 5(b)]. The shape of the central polygon (triangle, square, hexagon, etc) determines the rigid-foldability of the twist [94]. Twists have been used in applications such as conceal and reveal systems [95], as well as for research into self foldability of origami mechanisms [110].

Flasher patterns are a series of patterns that fold by rotating gores about a central polygon; these gore panels end up perpendicular (out-of-plane) to the central polygon (see Fig. 4). Flashers have been used for solar arrays [67] and diffractive telescopes [11]. Flasher patterns are not strictly rigid-foldable mechanisms, however, ways have been determined to create rigid-foldable flasher patterns [40], [99].

Other origami patterns have been used as inspiration for engineering work. Other prior papers have also reviewed how origami has been used in engineering, including [111]–[113].

A. MECHANICAL CONSIDERATIONS OF ORIGAMI TO ANTENNAS

Mechanical considerations that are important to origami antennas include nesting, thickness accommodation, stability, and deployment [114].

Thickness accommodation techniques are essential for thick origami mechanisms to allow for the kinematic equivalency of the thick mechanism to the zero-thickness model or at least a similar motion and endpoints. When patterns become thick, panels must nest inside each other, such as, the case with the Miura-Ori. To preserve the rigid-foldability of the panels while maintaining the range of motion, thickness accommodation techniques allow for this nesting to occur through the selection of appropriate techniques and joints [50]. While each of these methods may produce desirable results, they must be considered in concert with how each technique will affect the stability and the flatness of an origami antenna.

In antenna applications, the stability and flatness of the deployed mechanism is paramount. Research has been performed to identify ways to maintain the stability and flatness of a deployed origami mechanism. One approach to stability is the utilization of hard stops, which can be deployed from the thickness of the mechanism and allow the mechanism to lock in specific stages of deployment [115]. Regionally sandwiched compliant sheets (ReCS), with specific mountain-valley assignments, are used so that only one fold path can occur, aiding in stability by eliminating bifurcation points [116]. If variability of position is required, the stability of the joints must be adjustable. The use of shape memory polymer (SMP) joints has also been explored [117]. The stiffness of these SMP joints was adjusted through the use of a flexible embedded heater. Various kinds of compact directional and frictional hinges in foldable mechanisms are another potential option [118]. Each of these techniques can be used to improve the stability and flatness of origami antennas. Other methods may also be valid.

In these applications, maximizing the deployed area relative to the stowed volume is important. This is accomplished using thickness accommodation techniques and origami patterns that adequately deal with the nesting of panels to maximize the percentage of stowed volume used. For deployment, it is also important to consider how each antenna will be fixed to the base structure, such as a CubeSat or other satellite. Different types of connections may allow for different types of deployment (symmetric, in-plane, etc.). Additionally, the mechanisms that will be used to cause this deployment need to be considered. Previous methods have used inflatable trusses [119], magnetic actuation [120], foldable masts [80], and strain energy [97]. Each of these should be considered on the basis of the volume that the deployment mechanism will take, the need for energy input to actuate the mechanism, compatibility of the mechanism with thickness accommodation, stability, and flatness techniques used. The mechanical design of deployable origami antennas is a multi-faceted problem and the issues discussed here are often highly coupled and need to be considered together.

IV. ORIGAMI ANTENNAS REVIEW

Our group has conducted significant research to pioneer the development of origami antennas, e.g., [121]. Notably, our research on origami antennas has used geometric origami, computational tools and novel materials to demonstrate that origami enables the development of new electromagnetic systems with the following important capabilities.

1) 2-*D* and 3-*D* antennas that can morph their geometrical shape to control performance parameters as a function of time and achieve multifunctionality,
2) 2-*D* and 3-*D* antenna arrays that can change their footprint, shape, and/or element separation to achieve optimal beamforming, beamsteering, and scanning range, and
3) reconfigurable frequency selective surfaces for tunable and multifunctional antennas and arrays.

Fig. 6 summarizes the advantages of origami EM designs using some of the designs that we have presented before. The efficient packing of origami antennas is demonstrated on the left of Fig. 6 using an origami reflectarray on a CubeSat. This reflectarray can stow itself very compactly and when it reaches orbit, it can deploy itself to provide a large aperture. The easy deployment of origami antennas is shown on the second column from the left of Fig. 6 using a four patch element array. This array can deploy itself using a lamina emergent torsional (LET) hinge that can be monolithically manufactured on a thick substrate with the array [122]. The reconfigurability of origami antennas is demonstrated on the third column of Fig. 6 using a foldable loop antenna. This loop can fold itself at different states to reconfigure its pattern. Finally, the ability of origami designs to provide enhanced EM performance is illustrated on the right column of Fig. 6 using a Miura-Ori frequency selective

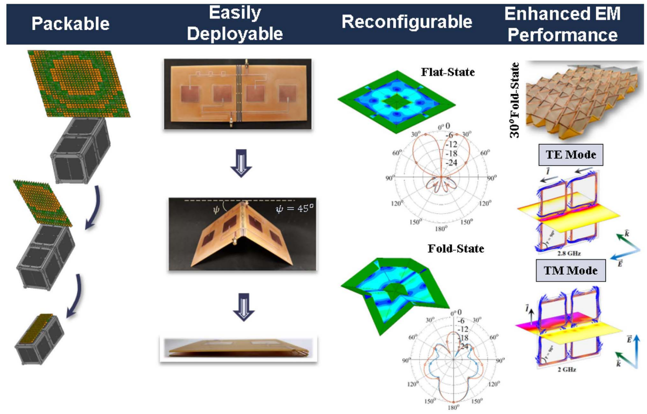

FIGURE 6. Advantages of origami antennas. From left to right: deployable reflectarray mounted on a CubeSat, four-element patch array printed on a deployable thick substrate, radiation pattern reconfigurability of a deployable loop antenna, dual-band origami FSS.

surface [123]. This origami-inspired FSS transforms a conventional single-band FSS design to a dual-band spatial filter by applying the Miura-Ori origami pattern on the FSS.

In fact, our work has aimed to use origami designs for antennas not only for packing purposes but also for enhancing their EM performance. Specifically, frequency, polarization, and radiation pattern reconfigurability can be achieved by physically morphing EM structures. Notably, origami mechanisms have unique advantages over other types of deployable mechanisms. Specifically, origami mechanisms have the ability to:

- create desired forms using planar fabrication processes, and
- create mechanisms with a large number of moving parts with a low number of degrees of freedom. What makes a mechanism an "origami" or "origami-inspired" mechanism is the presence of interior vertices, or in different language, coupled spherical mechanisms. This family of mechanisms strikes a balance between the generic overconstraint of general 3-D mechanisms and the generic underconstraint of linear or tree-like chains. By using origami mechanisms, we can achieve complex and/or precise motions in shape-shifting elements with a relatively small number of actuators, and thus a relatively simpler control system for deployment and/or stowage.

Here, we briefly discuss important works on EM origami designs, and in Section V we focus on the research that our group has conducted on origami antennas. A programmable metamaterial was investigated based on ternary foldable origami in the gigahertz regime in [124]. In this design, four transformable modes were shown corresponding to four different functions of electromagnetic reflector and frequency-selective absorbers. In [125], Ng and Young introduced a simple origami folding technique transforming a planar 2D antenna to a 3D array of Vivaldi antennas obtaining a gain of 8.27 *dBi* with circular polarisation. Njogu *et al.*, [126], presented dual-band inkjet printed planar monopole antennas integrated with an origami flapping bird (crane) structure; specifically, two antennas were built, one placed on the spine, and the other on the tail of the origami crane, improving coverage on a traditional communication system.

Furthermore, origami frequency selective surfaces (FSSs) were studied in [127]–[129]. The focus of these studies was on the selective transmission characteristics of folded surfaces loaded with periodic arrangements of split-ring resonators, and the tuning abilities of these designs by changing the folding states. Also, origami-inspired FSSs and their frequency and polarization dependencies on folding states were examined in [130], [131]. In addition, an origami-inspired parabolic reflector antenna was introduced in [132], and this work analyzed the effects of the size and shape of origami tessellations on the radiation performance of the reflector.

A smart shape-memory hinge, which can be fabricated in a flat state and later be folded into a 3D shape through heating, was presented in [133]. Specifically, the conductive traces in this design were fabricated using inkjet printing. Furthermore, a self-folding polymer, which responds to light, was used to convert a monopole antenna into a patch antenna [134]. In addition, a parabolic reflector antenna with smooth folding was developed in [135] by combining shape memory polymer (SMP) composites and self-folding origami techniques.

A tunable origami structure loaded with electrical components, which can be reconfigured over continuous-state ranges from folded to unfolded configurations, was developed in [136] using inkjet printing techniques. Also, a thermally actuated multilayer FSS, which achieved a continuous-range of tunability by using polyester-based substrates, was presented in [137]. Moreover, a bi-directional loop antenna on a single origami magic cube was designed in [138], where a series fed array with a realized gain of 5.53 dBi was formed using three cubes connected in series.

Several works, [139]–[141], also combined 3D printing with origami to develop antenna designs with very low fabrication cost. Specifically, 3D printed reconfigurable antennas were developed using liquid metal alloys and microfluids in [139]. A tree model was introduced in [140] to reconfigure the performance (frequency, polarization, and radiation pattern) of antennas with liquid metal alloys (i.e., EGaIn). Furthermore, a 3D printed flexible and reconfigurable bowtie antenna, which could tune its operating frequency by changing its apex angle, was introduced in [141]; in this work, liquid metal alloy was used to prevent breakage while folding.

A circularly polarized origami antenna based on orthogonally excited monopoles was presented in [142]; in this work, simple origami folding was used to orient two monopole antennas perpendicularly to each other and achieve circular polarization. Also, a paper-based Yagi Uda antenna was developed in [143] using three magic cubes to form its driven, reflector and director elements. Moreover, a bio-inspired quasi-Yagi origami helical antenna was developed in [144].

Several works have developed origami antennas for space applications. For example, a deployable conical log spiral and a quadrifilar helical antenna were presented in [145] using special conductive traces (based on beryllium copper or phosphor bronze) that were supported by reinforced epoxy (based on glass fiber or continuous fiber composites). More recently, a deployable reflectarray for CubeSats using the origami flasher geometry was proposed in [146], where PCB panels were appropriately cut to enable folding. Another origami-inspired reflectarray was designed in [147] using flexible materials and strereolithography 3D printing technology. Few works on origami antennas with thick substrates have also been presented. Specifically, a foldable patch antenna array on a thick 0.75 mm polypropylene substrate was developed in [148] by scoring the Miura Ori pattern on this substrate using a laser; however, this structure was able to fold only to a specific extend due to the thickness of the substrate. The work we presented in [122] solved this limitation by presenting for the first time a thick origami based antenna array that can fold/unfold for a range of 360 degrees without causing any mechanical or electromagnetic failures. Inspired by our work on thick origami, a similar approach was followed by Hwang *et al.*, [149], who developed a planar deployable dipole array that could reconfigure its radiation pattern from an omnidirectional to a broadside directive pattern. Finally, a microstrip patch antenna array on a thick foldable substrate was presented in [150]; this design used the Miura-Ori pattern, and the ground plane along with the feed network were modified to enable folding.

An accordion-based ground plane for a tightly coupled dipole array, and also a textile-based log periodic dipole array were presented in [151]. Also, a textile-based origami dipole antenna was developed in [152] using a conductive thread and applying $7E-threads/mm$ density with $1E-threads/mm$ at the creases to improve the foldability of the structure.

In the next section, we present the evolution of our research efforts on the development of origami antennas.

V. DEVELOPMENT OF ORIGAMI ANTENNAS

Traditional origami assumes that the folding material has zero thickness, and origami designs usually require modification when a finite thickness is added. Therefore, for simplicity and to follow existing origami designs, our first origami antennas were built on thin flexible substrates, such as paper, and Kapton® [153], [154]. Two such antennas are shown in Fig. 7. Specifically, Figs. 7(a) and 7(b) show an origami Yagi-Uda loop antenna [155], and an origami bifilar helical antenna [153], respectively. Both these origami antennas provided reconfigurable performance in terms of frequency by exploiting the folding/unfolding capabilities of origami. Also, they provided comparable performance in terms of input impedance matching and radiation efficiency to traditional antennas.

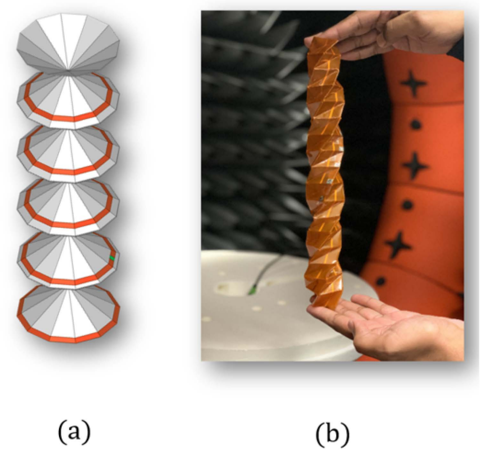

FIGURE 7. First origami antennas on thin flexible substrates: a) origami Yagi-Uda loop on paper, and b) origami bifilar helix on Kapton.

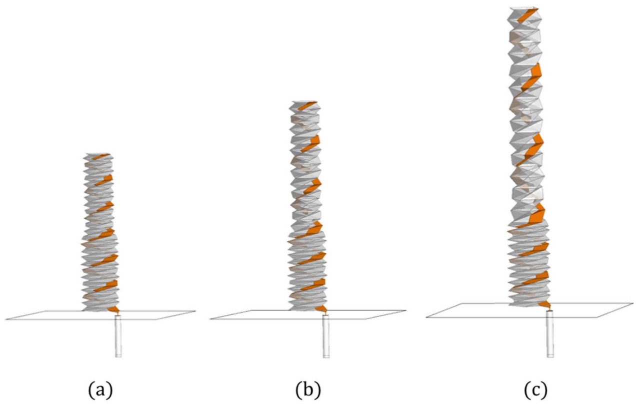

FIGURE 8. Multi-radii monofilar helical antenna operating at its three different folding states covering respectively: a) GPS, b) satellite radio communications, and c) WiMAX applications.

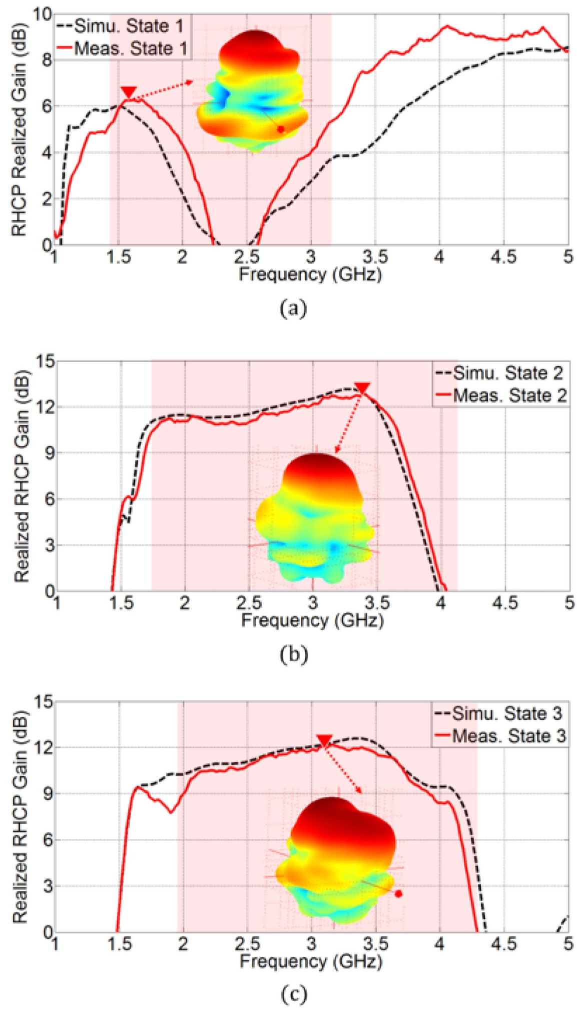

FIGURE 9. Gain of multi-radii monofilar helical antenna at its three different folding states: a) GPS, b) satellite radio communications, and c) WiMAX.

Also, we presented the first origami multi-radii monofilar helical antenna on paper substrate in [156], which operates in three different bands with circular polarization. Specifically, two helical antennas with different radii were embedded on a Kresling origami design that exhibited reconfigurable performance and efficient packing. Fig. 8 shows this design at its three states of operation, namely, GPS, satellite radio communications, and WiMAX. The corresponding performance of this origami antenna at the three states is shown in Fig. 9.

Paper-based origami antennas were easier to build in the early stages of our research. However, paper substrates have limited practical applications, since they can be easily damaged. In addition, certain polyimide-based origami antennas lack mechanical robustness, since after a relatively small number of folding/unfolding cycles ($50-150$ cycles depending on the thickness of the material), they experience cracks along the creases and near points of high stress.

Fig. 10 depicts an example of such failure of an origami helical antenna on flexible polyimide substrate. Furthermore, antennas often must withstand harsh environments and sustain extreme conditions, such as, abrupt temperature changes, wind, and rain. Such conditions can severely damage origami designs on thin flexible substrates by degrading their mechanical and electrical performance.

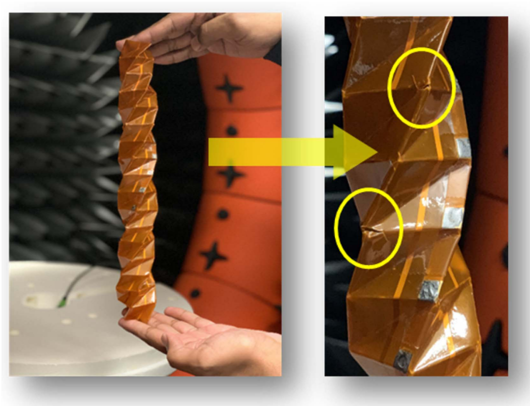

FIGURE 10. Polyimide-based helical origami antenna. The flexible substrate (polyimide) experiences fatigue after 50-100 cycles of folding/unfolding.

To address the above problems of origami antennas, we have introduced: (a) new material systems that can sustain

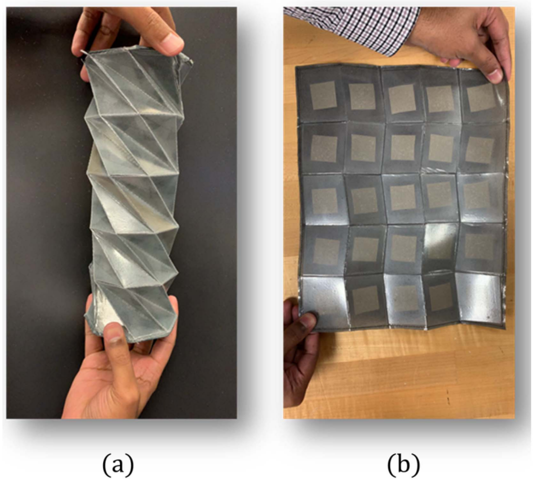

FIGURE 11. First multi-layer multi-material origami a) helical antenna, and b) FSS. This design approach provides robust operation reducing the stresses at the creases and corners, thereby eliminating cracking issues of previously introduced designs, such as the polyimide based antenna of Fig. 10.

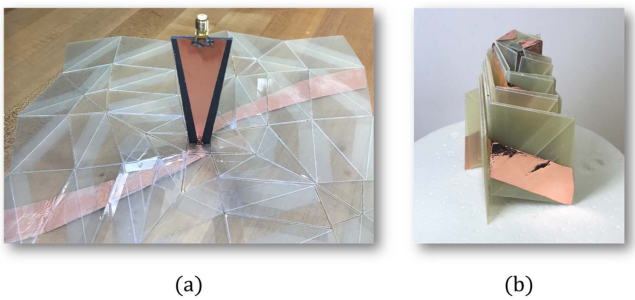

FIGURE 12. First thick origami antenna. The flasher model transforms a dipole antenna shown in a) to a conical spiral shown in b), thereby providing radiation pattern and frequency reconfigurability.

multiple cycles of folding/unfolding, and (b) origami antenna designs on thick and rigid substrates. First, we proposed a new multi-layer multi-material system for origami antennas in [157]. Two examples of such origami antennas are shown in Figs. 11(a) and 11(b), and they provide robust operation by reducing the stresses at the creases and the corners, thereby eliminating the issues with cracking. A complete description of this design approach along with new results are presented in Section VII.

Second, we developed rigidly foldable EM designs to provide robust operation in harsh environments. Specifically, we proposed a thick origami antenna [158], as shown in Fig. 12, based on a rigid origami flasher [40], that can transform a dipole to a segmented conical spiral antenna. This antenna uses thick panels (*FR*4 with a thickness of 32 *mil*) that are held in place using a flexible membrane. Therefore, it can be constructed using standard PCBs, which simplifies its manufacturing.

Our work on thick origami designs was further expanded by proposing both active and passive thick origami arrays. First, Hamza *et al.*, in [122] introduced a monolithic thick origami active array, as shown in Fig. 13. This array folds/unfolds over a range of almost 360° using a lamina

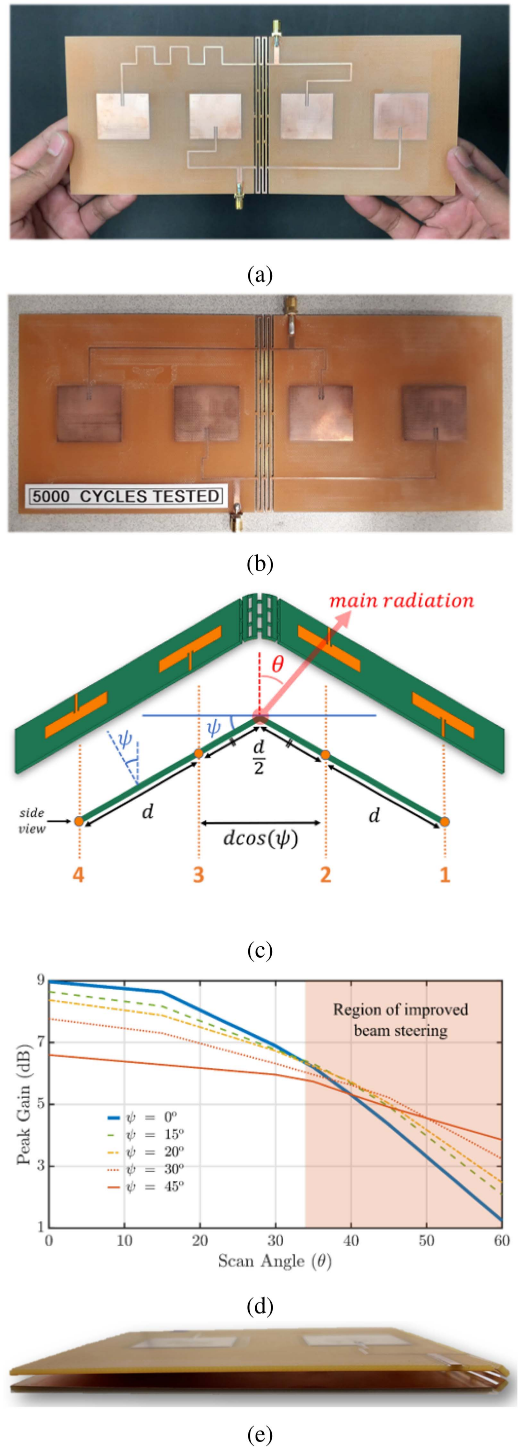

FIGURE 13. First thick origami array introduced by our group in [122]: a) Monolithic four element thick origami array including the antenna elements, feed network and hinge. b) The array maintains consistent mechanical and electromagnetic (EM) performance through 5,000 folding cycles of complete angular deflection (±180°) without any failures. c) Progressive phase calculation for our foldable four element patch array. d) This monolithic deployable array realizes improved beam steering capabilities for scan angles greater than 35°. e) When it folds, the array reduces its area to 50%.

emergent torsional (LET) hinge, [159]. The term monolithic refers to the fact that this design [including the antenna elements, feed network and hinge shown in Fig. 13(a)] can be

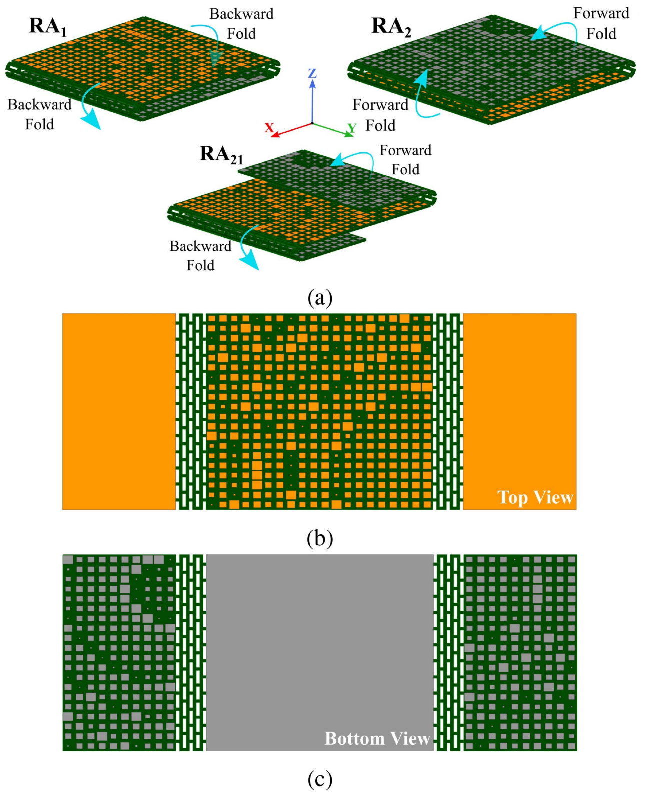

FIGURE 14. Foldable and reconfigurable monolithic RA at, a) different folding states RA_1, RA_2 and RA_{21}, b) top view and c) bottom view.

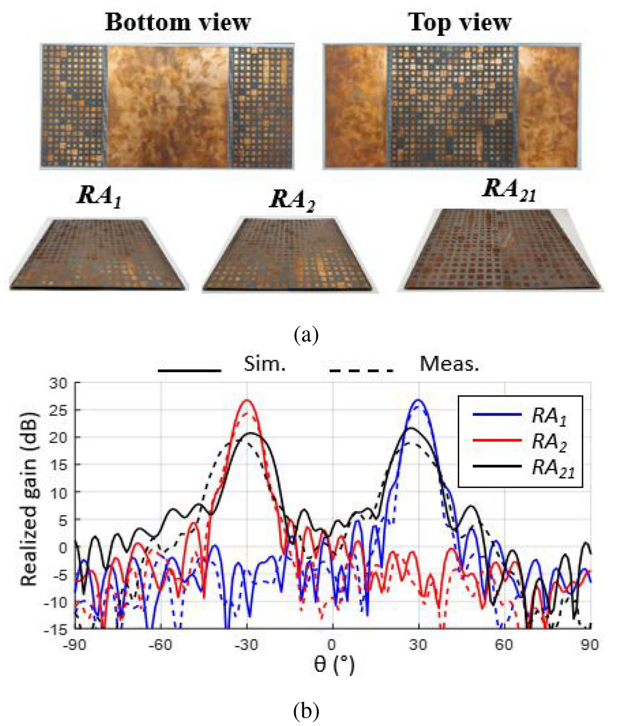

FIGURE 15. Foldable and reconfigurable monolithic RA [160]. a) Prototype. b) This RA's three different aperture sub-configurations with corresponding patterns.

manufactured in a single manufacturing step, thereby eliminating the need for assembly and additional mechanical parts. Also, the robustness of this origami array is exceptional, as it maintained consistent mechanical and electromagnetic (EM) performance through 5, 000 folding cycles of complete angular deflection ($\pm 180°$) without any failures. Figs. 13(c)-(d) show as this array changes from its planar to its non-planar state, it provides improved beamsteering capabilities for scan angles greater than 35°.

Second, aiming to space applications we have developed novel deployable reflectarrays by introducing three different design approaches; (a) monolithic designs using traditional PCBs, (b) multi-layer multi-material designs using thick substrates, and (c) multi-layer multi-material designs using additive manufacturing techniques.

Kaddour *et al.*, in [160] introduced a novel reconfigurable and monolithic reflectarray (RA) with foldable panels. This passive array is suitable for CubeSat applications targeting communications that require multiple directions, i.e., beam-scanning or radiation diversity. The proposed RA has extremely low fabrication cost, reconfigurable EM performance, beamsteering capabilities, efficient stowage, and excellent compatibility with CubeSat geometries. By folding and unfolding its panels, this high-gain RA can support three different aperture sub-configurations with three different patterns, namely, two single-beam patterns and one dual-beam pattern. The proposed design is shown in Fig. 14, and it consists of a combination of multiple RAs (RA_1, RA_2 and RA_{21}) that provide mechanically reconfigurable radiation properties (single and dual-beam) and beamsteering, while reducing the cost due to fewer parts, simplified manufacturing, and no need for maintenance. The key advantages of our proposed RA include (1) mechanical reconfigurability into multiple states, and (2) a LET hinge design that offers advantages over current folding mechanisms used in RA designs. Fig. 15(a) shows the fabricated prototype using standard PCB fabrication at its three different folding states RA_1, RA_2, and RA_{21}, and compares the simulated and measured realized gain patterns of the three sub-configurations in Fig. 15(b). Notably, this monolithic RA establishes a new type of RA that is well-suited for on-site manufacturing in space exploration missions, i.e., this RA can be made in space using simple and additive manufacturing processes.

Rubio *et al.*, in [161] expanded our multi-layer multi-material design and fabrication approach introduced in [157], to design RAs that utilize thick substrates. Namely, he introduced a novel RA composed of 15 PCB circuits, mounted on an origami-inspired foldable structure, which is called a straight-major square-twist (SMST) pattern [162], as shown in Fig. 16. This structure was designed to add stiffness to the RA structure, accommodate for material thickness, and enable the RA to fold in a way that exposes three different sets of RA panels. The thickness of the pattern shown also provides built-in stops that limit the motion and keep the panels parallel to each other. Each crease in the pattern is created using a Kapton® membrane hinge. This origami-inspired structure allows for the potential of multiple

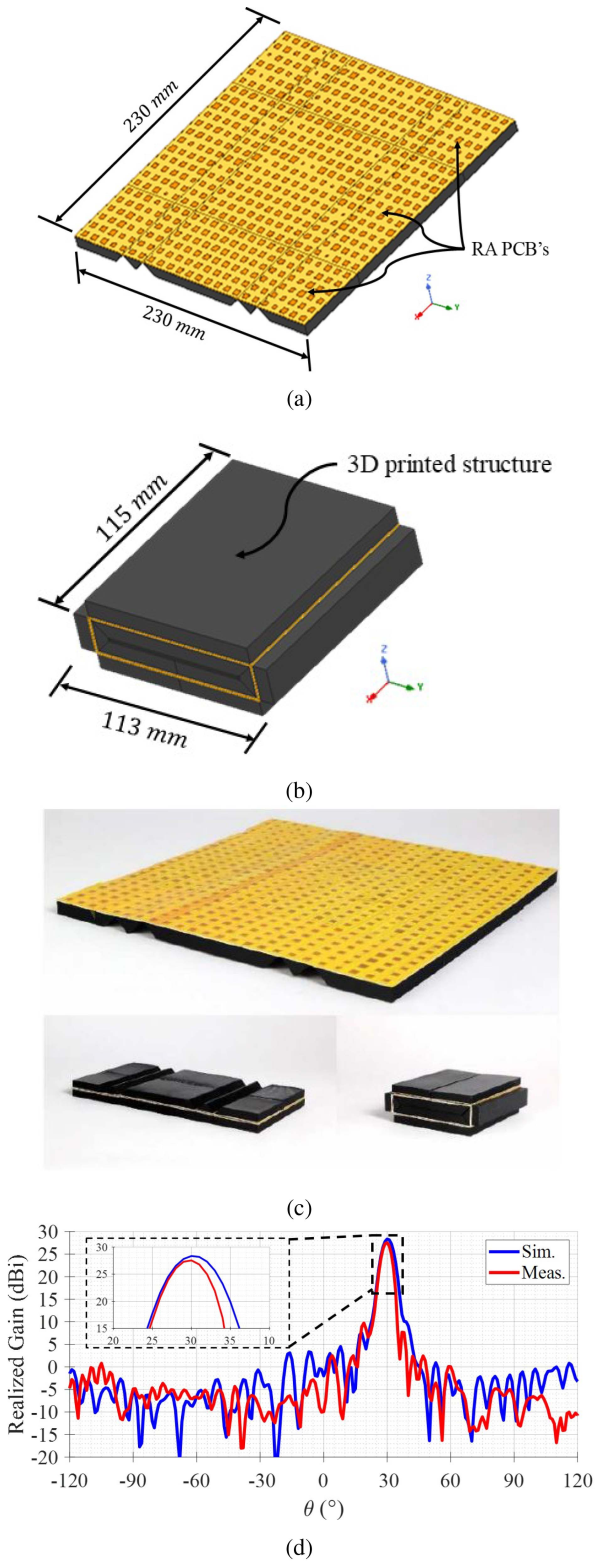

FIGURE 16. Reflectarray antenna on the straight-major square-twist structure [161]. a) Deployed state. b) Stowed state. c) Fabricated RA shown at its different folding states. d) Simulated and measured realized gain pattern at 16 *GHz*.

apertures. When not in use, the structure can be folded and stowed [Fig. 16(b)], and when in use, the array can be unfolded, as shown in Fig. 16(a). Figure 16(c) shows the three different states to which it folds. This pattern allows for a footprint increase from stowed to deployed configuration of more than 400% for a 1.0 *cm* panel thickness. This pattern also exhibits a volume packing efficiency of 92%, which increases as panel thickness decreases. Packing efficiency was determined as a ratio between the volume of the fully folded state and the volume of the smallest bounding cuboid of the fully folded state, respectively. The RA provides a pencil beam (directed at $\theta = 30°$, $\phi = 0°$) with a realized gain of approximately 28 *dBi* as seen in Fig. 16(d).

Finally, aiming to low-cost fabrication approaches, we have used additive manufacturing techniques for our multi-layer multi-material designs. Specifically, Kaddour *et al.*, in [163], presented a novel reflectarray unit-cell based on the Miura-Ori origami pattern. In this design, significant area reduction was achieved by a factor of 6, when the proposed reflectarray is stowed, compared to its unfolded state. Notably, the origami reflectarray antenna provides a reconfigurable behavior, i.e., its frequency of operation changes as it folds. This antenna has the potential to be applied in SmallSats, where efficient stowage is very important. The Miura-Ori unit-cell consists of a 3-layer design, as shown in Fig. 17(a). The first layer consists of four parallelogram patches printed on *RO*3010 substrate. Each patch is placed inside a cavity made of flexible Polypropylene material. The flexible Polypropylene section (second layer) is 3*D* printed and it supports the folding/unfolding ability of our design. Finally, a third layer (i.e., ground plane) is added using a thin metallized Kapton® substrate. The thickness of the ground plane is appropriately chosen such as to maintain the flexibility of the Miura-Ori unit-cell. This Miura-Ori unit-cell enables the reflectarray to achieve high packing efficiency. Fig. 17(b) shows several folding states of the proposed Miura-Ori unit-cell and its corresponding EM performance is shown in Fig. 17(c).

By folding the Miura-Ori unit-cell the physical size of the unit-cell decreases. Consequently, the operating frequency of the unit-cell shifts to higher frequencies as it can be observed in Fig. 17(c). Fig. 18 shows that this design achieves a maximum directivity of 17.5 *dBi* at 8.425 *GHz* with a 2 *dB* directivity bandwidth from 8.2 *GHz* to 9.4 *GHz* (13.6%). Notably, the maximum realized gain decreases as the reflectarray increases its folding angle. This is expected due to the following two reasons: (a) as the reflectarray folds, its effective area reduces, and (b) the elements are not perfectly synthesized for operation at higher frequencies. Furthermore, many other deployable [164], and reconfigurable [165], [166], origami RA designs have been proposed.

Origami antennas have been extensively used due to their packing abilities, easy deployable mechanisms, and reconfigurable features as they morph their shape. Moreover, as discussed in Section IV, origami designs also have the ability to provide enhanced EM performance compared to

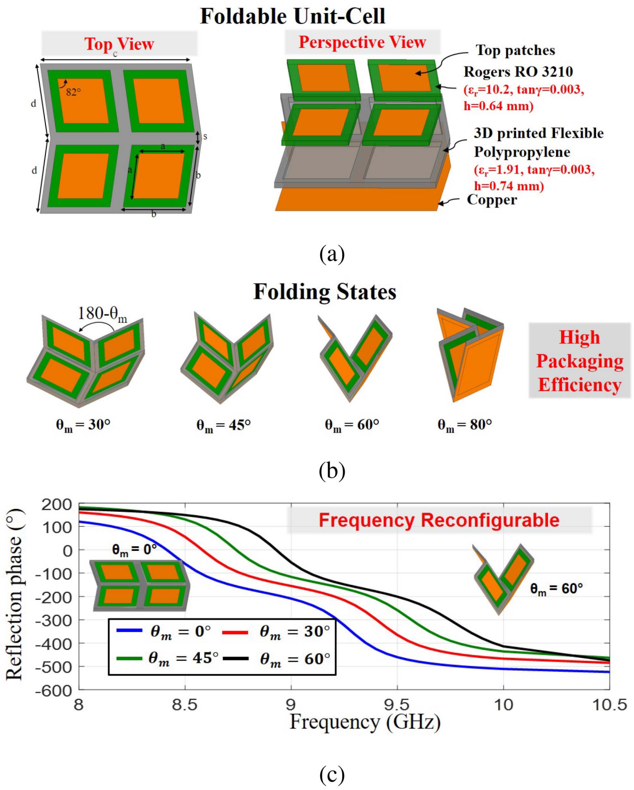

FIGURE 17. Miura-Ori reflectarray antenna[163]. a) Foldable unit-cell. b) Unit-cell at different folding states. c) Reflection phase and losses at different folding angles of the Miura-Ori reflectarray unit-cell.

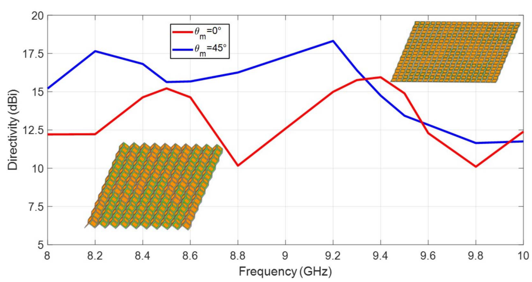

FIGURE 18. Miura-Ori reflectarray antenna performance. Gain pattern vs frequency for $\theta_m = 0°$ and $\theta_m = 45°$.

traditional electromagnetic designs. Biswas *et al.*, in [123], first illustrated this by developing a novel origami dual-band FSS [see Fig. 19(a)].

Namely, in [123], we showed for the first time that origami transforms a single-band static FSS to a dynamic dual-band FSS by conforming periodically spaced electromagnetic resonators to a Miura-Ori folding pattern (see Fig. 20).

Unlike the typical complicated multi-layer FSSs designs, the presented origami-FSS is simple and can be easily used from microwave to optical frequencies. Notably, designing multi-band electromagnetic structures with minimal design complexity and fabrication cost is very important for numerous applications, such as radar cross-section, radomes, artificial electromagnetic bandgap structures, etc.

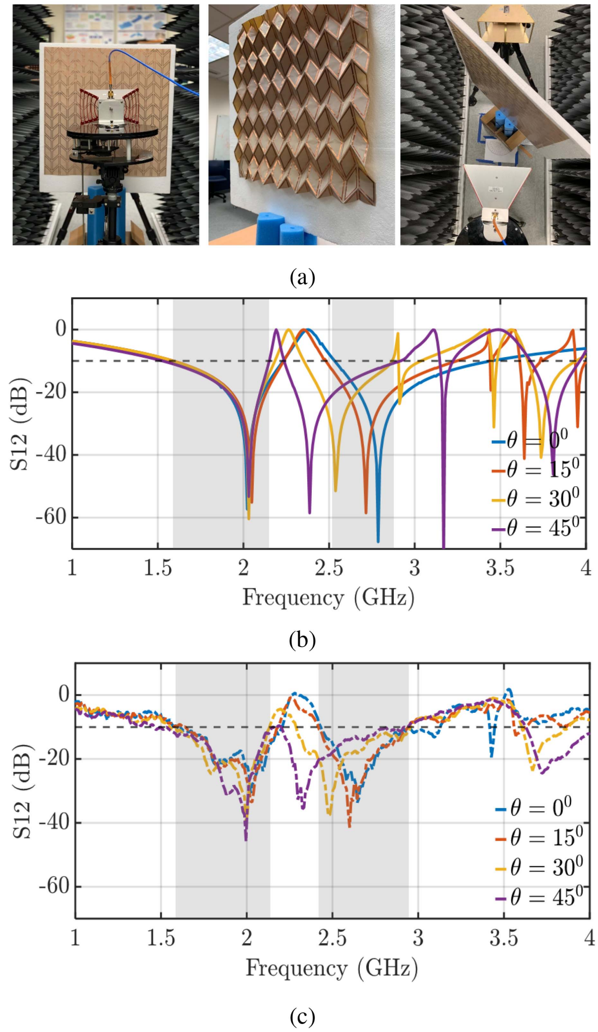

FIGURE 19. Dual-band origami FSS: a) Measuring our FSS prototype. b) Simulated results, and c) measured results.

VI. ORIGAMI ANTENNAS TOOLSETS

Due to their complex geometries, origami antennas face unique design challenges, compared to traditional EM structures. Modeling the kinematics of these structures along with their mechanical and electromagnetic performance at different folding-angles (or folding-states) is very difficult. Namely, when an EM origami design is developed, its behavior at different folding-states must be studied and appropriately optimized, if physical reconfiguration is one of the design goals. Several origami mathematical tools, that provide different origami patterns [58]–[62], [167]–[169], and simulate how origami patterns fold [59], [61], have been developed. However, there has been a significant lack of EM tools that can simulate EM origami designs in an automated way. To address this need, we recently introduced a toolset for automated modeling of origami EM structures in [170] (see Fig. 21).

In this toolset, origami math are used to generate any desired origami model. Then, thin models are converted

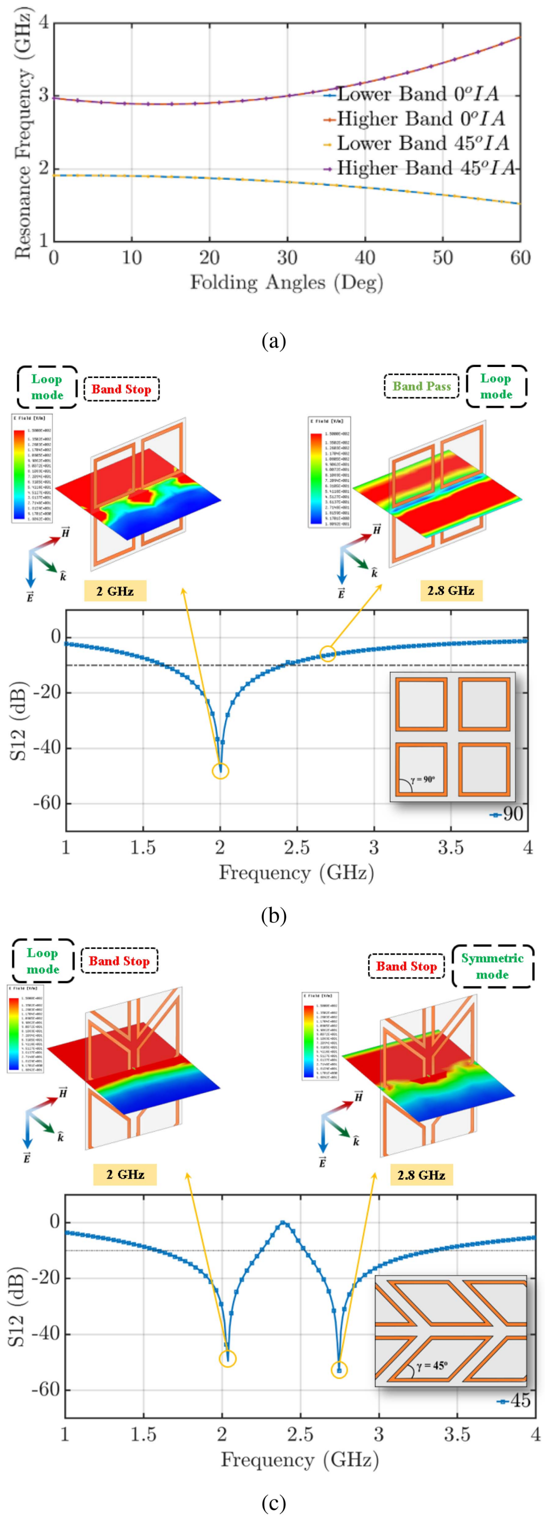

FIGURE 20. Dual-band origami FSS: a) Frequency reconfigurable behavior due to the deployable abilities of the origami FSS for a TE polarized impinging wave. b) Reflection coefficient and corresponding field distribution for the conventional single-band FSS. c) Reflection coefficient and corresponding field distribution for the dual-band origami FSS.

to thick, if needed, and the corresponding conductive and non-conductive (e.g., substrate, superstrate, etc.) areas are defined. The design in turn is analyzed in ANSYS HFSS,

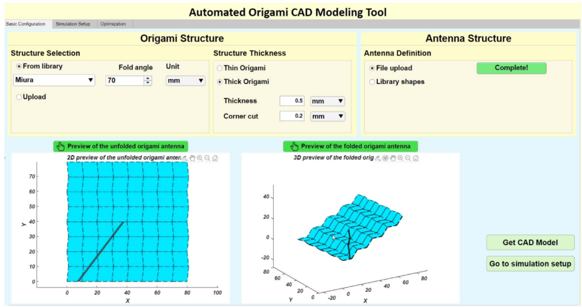

FIGURE 21. Graphical user interface of the first EM origami toolset presented in [170].

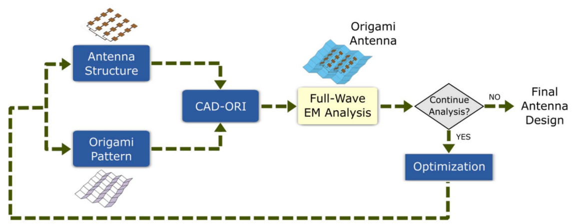

FIGURE 22. Toolset for modeling, analyzing, and optimizing origami antennas and EM structures.

and optimized based on the user's objectives. Below, a brief demonstration of this first EM origami toolset is given. A complete analysis can be found in [170].

As discussed in Section III, one of the unique characteristics of origami EM structures is their physical reconfiguration; a property that increases the analysis complexity. EM origami designs are physically reconfigurable since they deform their shape as they fold/unfold. Thus, the folding pattern (e.g., substrate) and the conductive area (e.g., antenna, filter, etc.) must be appropriately determined so that the EM origami design operates efficiently across its different fold-states. Therefore, a toolset that can model, simulate, and optimize origami antennas in an automated way is needed. The toolset we presented in [170] is the first of its kind that fulfills this purpose. To generate origami patterns, existing origami-math software (i.e., Tessellatica [61]) was used to create mathematically accurate CAD models. Also, the standard flexible origami list data structure (FOLD) format was utilized to generate all the required vertex, edge and face related information. This information offers essentially the origami kinematics as the structure transforms from one folded state to another. The flowchart for our toolset is shown in Fig. 22.

After the origami information is loaded, the EM design is mapped on the origami pattern. Notably, since a realistic EM design is comprised of both conductive and non-conductive materials (e.g., substrate), the origami design must have some realistic thickness. Thickness in origami designs is one of the biggest challenges and most of origami toolsets do not offer patterns for thick origami. To overcome this limitation, we tackled this challenge in [170] by introducing the desired thickness on any imported origami pattern. After

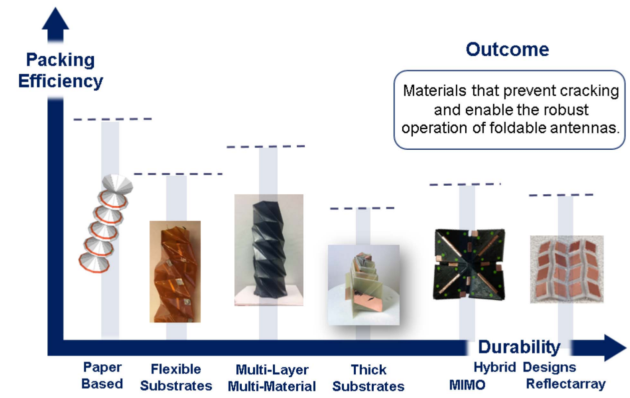

FIGURE 23. Evolution of EM origami designs in the last 5 years of research.

the EM origami structure is designed, full-wave analysis is performed. Finally, our toolset provides, as shown in Fig. 22, a module for optimizing the origami designs based on set design goals.

VII. DESIGN PROCESS AND ANALYSIS OF A NOVEL ORIGAMI ANTENNA

As discussed above, significant research has been conducted on origami antennas. Figure 23 shows the evolution of EM origami designs, starting from the design of antennas on thin substrates (e.g., paper and polyimide) and moving to designs with flexible, thick, and rigid materials.

In this work, we describe the design process and analysis of packable and reconfigurable helical origami antennas based on multilayer and multi-material systems. The multilayer and multi-material system is chosen as it enables the development of: (a) novel origami antennas with reliable and repeatable operation, and (b) new foldable antenna designs based on various manufacturing methods (e.g., additive manufacturing) and a combination of flexible (e.g., the third antenna from the left in Fig. 23) and rigid (e.g., the fifth antenna from the left in Fig. 23) substrates. This work is important as helical antennas are widely used in both terrestrial and space applications. Due to our novel design, our proposed origami helical antennas can sustain thousands of folding/unfolding cycles without breaking or cracking, while maintaining stable electromagnetic performance. In the next subsections, we briefly describe the design principles of an origami helical antenna (Section VII-A), identify the origami design principles (Section VII-B), demonstrate in detail the fabrication process (Section VII-C), and present both our simulated and measured results (Section VII-D).

A. DESIGN PRINCIPLES OF QUADRIFILAR HELICAL ANTENNA

Helical antennas were first investigated in 1947 by Kraus, [171], and Wheeler, [172]. Wheeler demonstrated that a helical antenna whose length is less than a wavelength behaves as a dipole with a coaxial doughnut shaped radiation pattern, while Kraus discovered the axial mode radiation, which is achieved when the circumference of the helix is close to a wavelength. Helical antennas are very well suited for various applications due to their high gain and circular polarization.

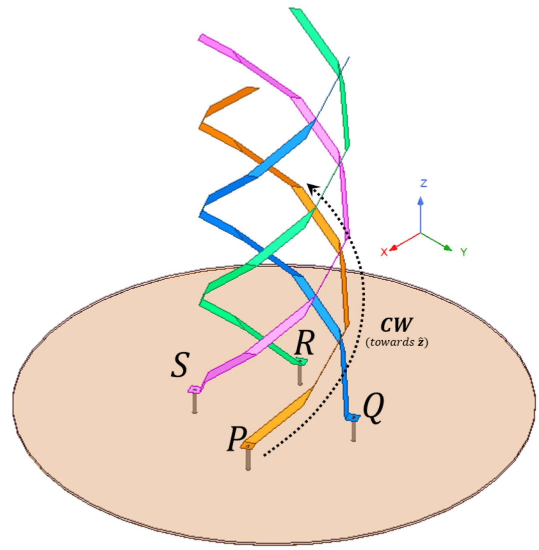

FIGURE 24. Quadrifilar helical antenna (QHA).

Helical antennas appear on cylindrical, conical, and spherical shapes with the main parameters setting their radiation characteristics to be: (i) the number of filaments wounded to form the corresponding shape, (ii) the diameter of the loops the filaments form, and (iii) the number of turns. When one filament is wounded, the helix is usually called monofilar, while when four filaments are used it is referred as quadrifilar helical antenna (QHA). QHAs require less number of turns compared to monofilar designs, which makes them better-suited for applications where space requirements are stringent. Therefore, we pick here to design an origami quadrifilar helical antenna (see Fig. 24).

The operation of a quadrifilar helical antenna, similar to the traditional monofilar one, is determined by the choice of the circumference (C_λ) in wavelengths, diameter of the ground plane (D_g), pitch angle (ψ), trace width (W), number of turns (N), and length of the trace (L). Namely, for operation in the axial mode, its circumference should lie between 0.4λ and 2.0λ, its pitch angle between 40° to 45°, and its ground plane should be 2.5 to 5 times the diameter of the helix (D) with the optimal value to be about $3.5D$, [173]. Note that if the C_λ is not appropriately chosen, the QHA radiates in the backfire direction ($0.35\lambda < C_\lambda < 0.45\lambda$), while for $C_\lambda > 1.6\lambda$ the beam patterns begin to deteriorate due to the presence of a scanning mode which appears first as high sidelobes and eventually leads to a complete pattern breakup for C_λ close to 2.7λ. The bandwidth of the QHA is mainly dependent on the number of turns (N) of the helix. For ultra-wideband (UWB) behavior, the number of turns is usually $N \geq 3$, and for narrowband behavior the number can be significantly reduced close to $N = 1$. All the QHA design parameters are tabulated in Table 1.

TABLE 1. QHA Design Parameters.

Parameter	Value
Circumference	$0.75\lambda \leq C_\lambda \leq 1.35\lambda$
Pitch angle	$40° \leq \psi \leq 45°$
Number of turns	$1 \leq N \leq 2$ (narrowband) $N > 2$ (wideband)
Ground plane diameter	$D_g \geq 3.5D$

*D: diameter of the helix

Also, a critical design parameter is the excitation. QHAs are fed with four excitations of equal amplitude and 90° phase difference, which are progressively applied in either a clockwise (CW) or counter-clockwise (CCW) fashion. In the case where there is no ground plane, the phase progression combined with the wire winding direction dictates the CW or CCW polarization as well as the antenna operation as endfire or backfire. When ground plane is used, the antenna always radiates at the endfire direction with right-hand circular polarization (RHCP) when both the phase progression and the wire winding direction are CW (as we look at the helix from a top view), and left-hand circular polarization (LHCP) when one of the two follows the opposite direction (e.g., CW for the wire winding direction and CCW for the phase progression).

B. DESIGN PRINCIPLES OF ORIGAMI QUADRIFILAR HELICAL ANTENNA

In this work, following our previous studies (e.g., [157]), the Kresling origami pattern is used for the design of our origami helical antenna. Taking into consideration the design parameters from Section VII-A, we combine appropriately the origami pattern with the helix as shown in Fig. 25.

Figure 25(a) shows the QHA on its planar state, with traces on the desired Kresling pattern. Figure 25(b) shows the origami QHA when the origami pattern on Fig. 25(a) is folded. Notably, the four conductive traces, depicted with orange color, are placed along the diagonal lines in the parallelogram unit [Fig. 25(a)], so that the desired pitch angle of 45° is achieved when the origami pattern is folded.

Figure 26 shows the Kresling origami pattern unit-cell. Aiming for a mechanically robust design, the dimensions a and b are appropriately chosen such that their ratio lies between 0 and $n/4$ [174], where n is the number of sides used to discretize the circular cross section of our helix, as shown in Fig. 25(a),

$$0 < ratio < n/4, \quad \{n > 4\} \tag{1}$$

Also, to achieve the desired EM performance, an optimal circumference C_λ is chosen along with the corresponding QHA's diameter D. These two values dictate the length a, therefore, b is chosen to satisfy (1). The next parameter to be defined is the length of each conductive trace. This length is calculated as the product of side length c (see Fig. 26) and the number of unit-cells m used. In our design, $m = 4$ as shown in Fig. 25(b).

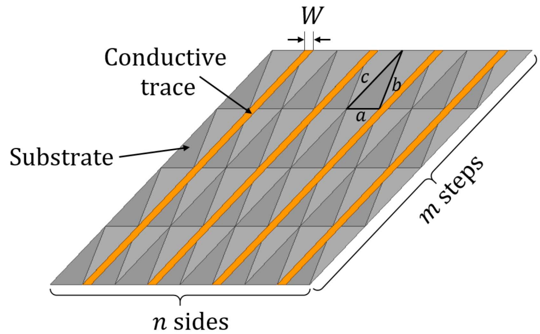

(a)

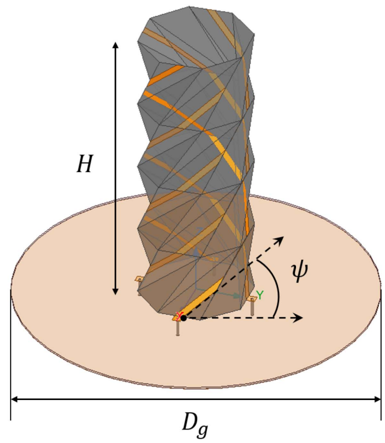

(b)

FIGURE 25. Origami QHA. a) Origami pattern with the traces for the proposed QHA, and b) helical antenna fully expanded operating at its axial mode.

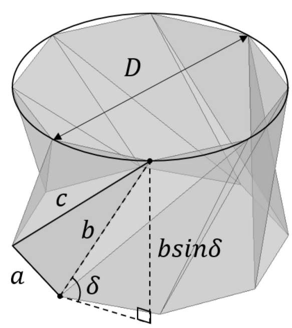

FIGURE 26. Unit-cell of a Kresling origami structure when is folded.

Note here, that theoretically the maximum height of the Kresling pattern is $m \cdot c$ (considering fully expanded case, i.e., $\delta = 90°$). However, a practical Kresling design is limited by the increasing stress on the edge c during deployment. Therefore, there is a theoretical maximum for the angle δ that can be calculated for a particular value of b and a. Hence, the height of the Kresling origami QHA varies with the angle delta as,

$$H = b \times sin\delta \tag{2}$$

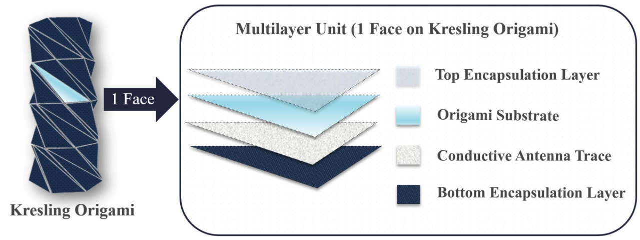

FIGURE 27. Multi-layer multi-material configuration for our origami quadrifilar helical antenna.

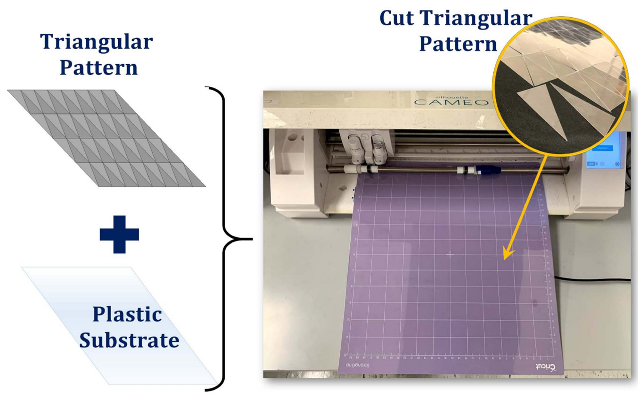

FIGURE 28. A Silhouette Cameo 3 cutting machine is used to cut the plastic film (origami substrate) according to the desired crease pattern.

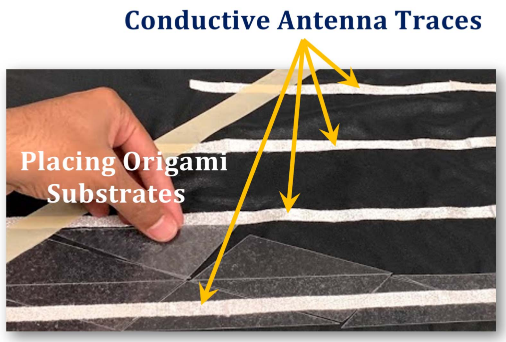

FIGURE 29. Conductive thread sewn on the fabric following the pattern of Fig. 25(a) and cut triangular pieces (which form the origami substrate) are appropriately placed on the sewn antenna.

Hence, the maximum height of the Kresling is given by,

$$H_{max} = b \times sin\delta_{max} \quad (3)$$

The maximum angle after deployment can be estimated by calculating the elastic strain of the truss model of cylindrical Kresling shell while unfolding, [174]. The deployment angle at which the elastic strain is minimized corresponds to δ_{max}. A very detailed analysis for the design procedure of a helical antenna on Kresling pattern can be found in [156].

C. FABRICATION PROCESS OF QUADRIFILAR HELICAL ANTENNA

As discussed in Section IV one of the main challenges on the design of origami antennas is their mechanical robustness. Notably, some of the first origami antenna designs experience cracks along the creases and near the points of high stress. Therefore, novel design and fabrication methods are needed to address this problem. To this end, we introduce here a novel multi-layer multi-material system for origami antennas. A general description of this novel fabrication technique can be found in our recently issued patent, [175]. Fig. 27 shows in detail the configuration of our proposed multi-layer multi-material system. Notably, this system in not limited to the specific types of materials and number of layers shown in Fig. 27 and the ones used in this work for our origami helical antenna.

A textile substrate with a conductive thread sewn on it are chosen as key elements of our proposed multi-layer multi-material system for our origami QHA to provide a robust and lightweight design, which does not crack when it is folded. In what follows, we describe step-by-step the manufacturing process of this system.

Step 1: The fabrication process starts by designing the crease pattern in our origami substrate. Here a plastic film of 0.007″ thickness is used as our origami substrate, as shown in Fig. 27. Traditionally, to design a crease pattern on a rigid substrate, material is appropriately removed by etching, scouring, or perforating the origami substrate. However, as mentioned in Section V, origami designs experience cracks along the creases and near points of high stress after multiple cycles of folding/unfolding. To eliminate this possibility of cracking, we follow here a new approach. Namely, we cut our rigid substrate into pieces, and completely separate them, according to the desired crease pattern. Figure 28 shows how we cut our plastic film in pieces using a Silhouette Cameo 3 cutting machine. In the inset of the same figure the triangular pieces of the Kresling pattern are shown.

Step 2: The next step is to design the conductive parts of our antenna as showed above in Fig. 25(a). Aiming to a crack-free foldable antenna design, a 0.04 mm thick Elektrisola $TW-0$ silver-coated copper conductive thread ($Cu/Ag50$), [176], is used as our conductive antenna trace. To keep in place the conductive traces, a lightweight water-proof fabric (Prosoft Eco-PUL W-578) is used, playing the role of the bottom encapsulation layer shown in Fig. 27. The conductive traces are sewn on the fabric following the design principles described in Section VII-B. Figure 29 shows the conductive threads as they have been sewn on our fabric.

Step 3: After the antenna design is completed we put together our radiator (the outcome of Step 2) with the origami substrate (the outcome of Step 1). This process is shown in Fig. 29, where all the plastic pieces are placed on top of the sewn antenna according to the pattern of Fig. 25(a).

Step 4: To keep in place the plastic pieces, we add adhesive material (i.e., glue spray) on their top face, as shown in Fig. 30(a), and we cover them with a thin plastic film shown in Fig. 30(b). The thin plastic film plays the role of the top encapsulation layer described in Fig. 27. The entire design is now sandwiched between the top encapsulation layer (our

(a)

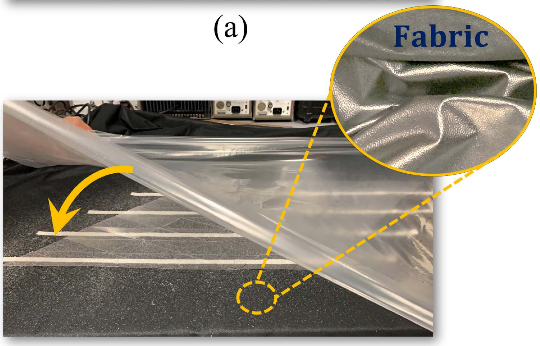

(b)

FIGURE 30. **(a) Spraying glue on the top face of our cut triangular pieces (origami substrate) as they are resting on the sewn antenna. (b) Placing the top encapsulation layer (our transparent plastic film) on the sewn antenna.**

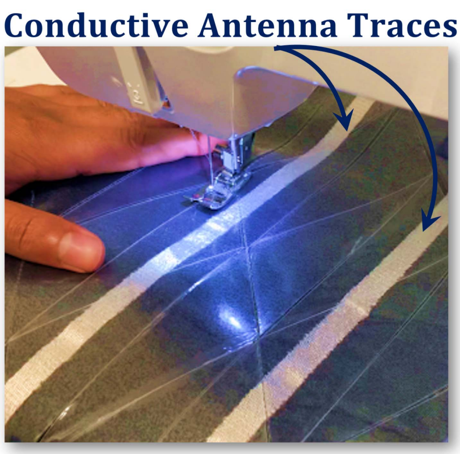

FIGURE 31. **Sewing the borders of each triangular piece on the textile substrate.**

FIGURE 32. **Folding appropriately and then hand-stitching the edges to form the desired origami Kresling pattern.**

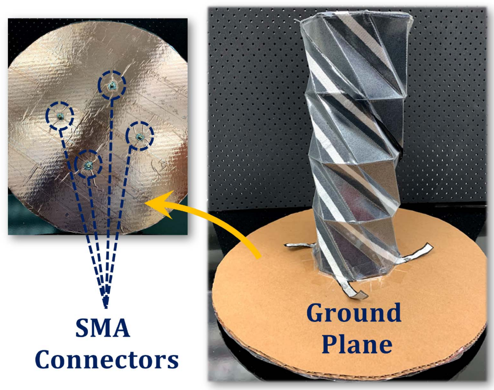

FIGURE 33. **Prototype origami QHA with the ground plane and feed (inset).**

TABLE 2. **Origami QHA Design Parameters.**

Parameters	Value	Parameters	Value
a	52.04 mm	N	1
b	101 mm	n	8
c	129.50 mm	m	4
D	136 mm	ψ	45°
H	344.48 mm	δ	58.50°
D_g	428.5 mm	W	10 mm

thin plastic film) and the bottom encapsulation layer (our fabric).

Step 5: Even though our origami substrate is held in place between the two encapsulation layers one additional step is applied to secure its position. Namely, using a standard sewing machine we sew the borders of each triangular piece on the textile substrate, as shown in Fig. 31. After this step we have a multi-layer multi-material origami structure that we can fold to form our intended origami Kresling pattern (see Fig. 32).

Step 6: After we fold the Kresling pattern, we hand-stitch it to form our origami helical antenna, as shown in Fig. 32. Notably, all the gluing and stitching during our manufacturing process must be carefully done to minimize spaces between the pieces that form the origami substrate.

Step 7: A circular cardboard covered with copper tape is placed at the base of our origami QHA antenna to form the ground plane. To feed the antenna four SMA connectors are soldered, as shown in the inset of Fig. 33. Our completed origami QHA is shown in Fig. 33.

D. RESULTS OF QUADRIFILAR HELICAL ANTENNA

Following the design guidelines of Sections VII-A and VII-A, our origami QHA is designed to operate at 421 *MHz* with all its parameters defined in Table 2.

First the antenna is numerically analyzed in ANSYS HFSS. As discussed in Section VII-A our origami antenna is excited by four feeds (e.g., four wave ports on HFSS) of equal amplitude and 90° phase difference, which are progressively applied in a CW fashion. Figure 34 presents the

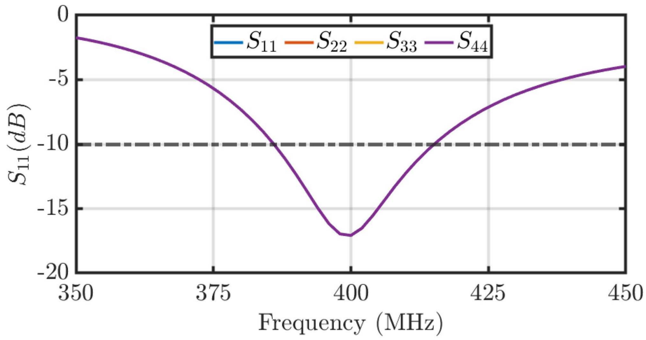

FIGURE 34. Simulated active S-parameters of the origami QHA.

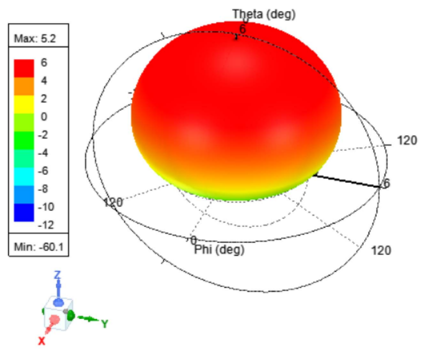

FIGURE 35. Simulated 3D radiation pattern of origami QHA antenna.

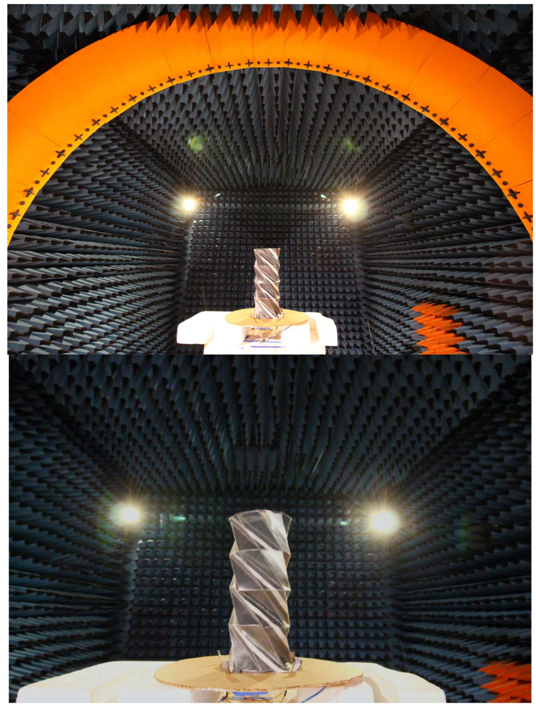

FIGURE 36. Proposed origami QHA antenna inside the *MVG SG*-64 near-field measurement system.

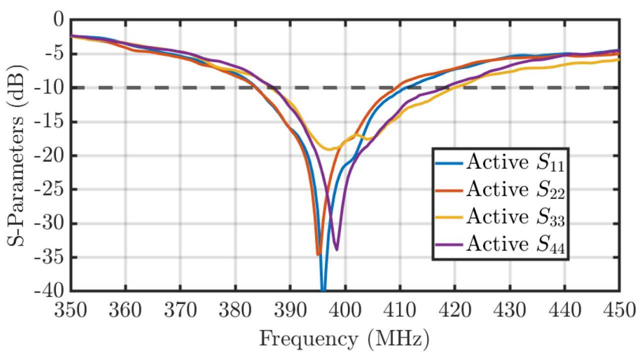

FIGURE 37. Measured active S-parameters.

simulated active *S*-parameters showing excellent matching at 400 *MHz* and an expected narrow bandwidth of 30 *MHz* within the range of 386-416 *MHz*. The 3*D* radiation pattern at 400 *MHz* is shown in Fig. 35.

The proposed origami QHA was measured using an *MVG SG*-64 near-field measurement system as shown in Fig. 36(c). To appropriately excite the QHA, a $0° - 180°$ and two $0° - 90°$ phase shifters were used to create a 90° difference between each arm. The measured properties of the fabricated feeding system have been introduced in the EM simulator.

Fig. 37 shows the active reflection coefficient for all four ports well matched at 400 *MHz*. A slight shift in the frequency of operation is seen due to fabrication tolerances.

The simulated and measured radiation and AR patterns at 400 *MHz* for both $\phi = 0°$ and $\phi = 90°$ plane cuts are shown in Fig. 38(a) and Fig. 38(b), respectively. It is observed that the patterns in the $\phi = 0°$ and $\phi = 90°$ planes are similar to each other and the radiation patterns of RHCP is symmetric for the maximum radiation direction. The co-polar (LHCP) field is stronger than the cross-polar (RHCP) counterpart by at least 15 *dB* over a wide range of elevation angle θ, giving a wide 3-*dB* AR beamwidth. The measured max gain is 4.5 *dBic*. This value is only 0.7 *dB* less compared to our simulated results, a deviation that occurs due to fabrication and near-field measurement tolerances. Finally, the simulated 3-*dB* AR beamwidths for $\phi = 0°$ and $\phi = 90°$ plane cuts are 162° and 150°, respectively, while the corresponding measured values are 72° and 78°. This difference in beamwidth is due to the high cross polarization level for $\theta > 30°$ and $\theta < -30°$. Overall, our results show a very good agreement between simulations and measurements.

Figure 39 shows the prototype at its fully expanded [Fig. 39(a)] and at its fully stowed state [Fig. 39(b)]. The volume of this antenna at its folded state is ~ 7.5 times less than its volume at its fully expanded state, therefore, this design provides excellent packing efficiency for applications where space is limited (e.g., space-borne applications).

Our multi-layer multi-material fabrication approach addressed one of the biggest challenges of origami electromagnetic structures, i.e., cracking after folding/unfolding. This approach is not limited to origami helical antennas and it can be used to manufacture other types of origami antennas. Also, other types of materials and different numbers of layers can be employed. As we demonstrated, our

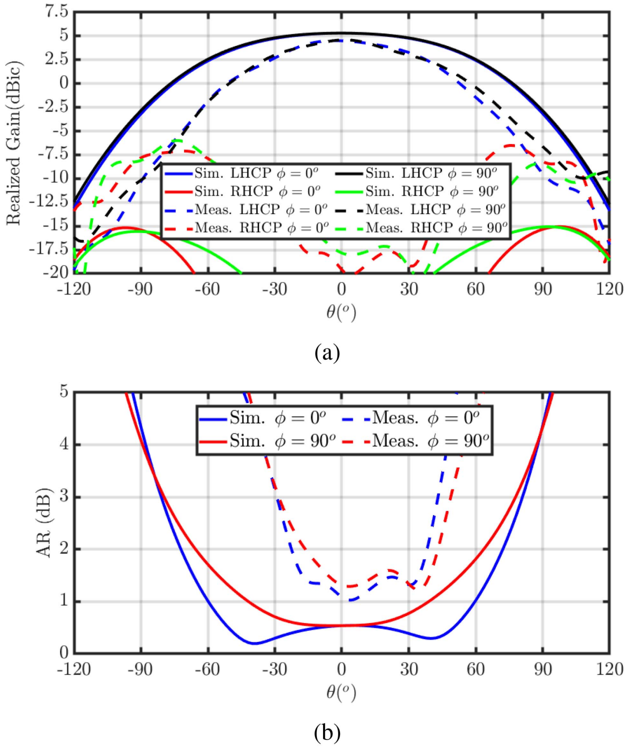

FIGURE 38. Comparison of simulated and measured (a) realized gain and (b) AR at 400 MHz in both planes $\phi = 0°$ and $\phi = 90°$. (a) (b)

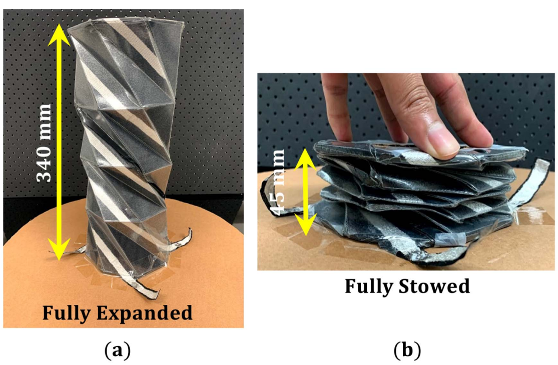

FIGURE 39. Packability of origami QHA. (a) Fully expanded view. (b) Fully stowed view.

origami antenna provides robust mechanical and electromagnetic performance. Moreover, even though this antenna was designed to operate at its fully deployed state and at only one frequency band, our proposed fabrication approach can be used for reconfigurable origami antennas that operate at multiple states and frequencies. For example, by folding and unfolding origami helical antennas they can operate at different states, [153].

VIII. DISCUSSION

Reconfigurable, tunable, multifunctional, deployable, and UWB high-performance antenna systems have been extensively used to provide multiple services to wireless communication systems. Electrical and mechanical reconfiguration methods have been developed and applied in numerous applications, such as, communications, reconnaissance, sensing and energy harvesting for airborne and spaceborne systems. Origami antennas is a new family of physically reconfigurable antennas that has been recently introduced, and they exhibit unique advantages over traditional antennas, such as performance reconfiguration, tunability, and efficient stowing. The inherent electromagnetic and mechanical multifunctional behaviors of origami antennas make them suitable for terrestrial and space applications, since they can be easily carried and effortlessly deployed. Also, the ability of origami antennas to morph their shape enables the development of new electromagnetic (EM) systems with unprecedented and transformational capabilities, among them: 1) antennas that can change their geometrical shape to control performance parameters as a function of time and achieve multifunctionality, 2) 2-*D* and 3-*D* antenna arrays that can change their footprint, shape, and/or element separation to achieve optimal beamforming, beamsteering, and scanning range, and 3) reconfigurable frequency selective surfaces for tunable and multifunctional antennas and arrays.

In this paper, we shed light on origami antennas by presenting the evolution of this unique technology. Starting from the design of antennas on thin substrates (e.g., paper and polyimide) and moving to designs with flexible, thick, and rigid materials (see Fig. 23), it can be concluded that the foundation for the design of origami antennas and EM structures has been already established. We anticipate that in the next few years, new game-changing origami antennas and electromagnetic structures will be introduced. These designs will maintain robustness as they dynamically actuate, fold/unfold, morph and/or reshape to enable tunable and reconfigurable EM operation, including RF matching, frequency reconfiguration, beamforming and controllable reflectivity. New mechanisms will also be designed that will enhance the capabilities of origami EM structures. Finally, to appropriately study the mathematical, mechanical and electromagnetic complexity of origami EM designs, unified computational design/optimization tools with multi-physics, origami math, and multi-scale modeling algorithms will be further developed.

IX. CONCLUSION

Foldable and physically reconfigurable antennas, particularly origami-based antennas, as shown in this work exhibit unique characteristics, such as multifunctional electromagnetic utility, ultra-compact stowage, deployment ease, and reduced weight. Their inherent electromagnetic and mechanical multifunctional behaviors make them suitable for terrestrial and space applications, since they can be easily carried and effortlessly deployed. However, designing these antennas is a challenging and multidisciplinary effort requiring the collaboration of researchers that span different fields including mathematics, material science as well as electrical and mechanical engineering. We anticipate that in the coming years origami antenna technologies and their design tools will further advance and mature, thereby leading to game-changing designs that will benefit various commercial and military applications.

ACKNOWLEDGMENT

The authors would like to thank MVG, INC, Marietta, Georgia for assisting them with the measurements of the origami quadrifilar helical antenna.

REFERENCES

[1] J. Anguera, C. Puente, C. Borja, and J. Soler, "Fractal shaped antennas: A review," in *Encyclopedia of RF and Microwave Engineering*, vol. 2. Hoboken, NJ, USA: Wiley, 2005, pp. 1620–1635. [Online]. Available: https://onlinelibrary.wiley.com/doi/abs/10.1002/0471654507.eme128

[2] "The history of paperfolding: A German perspective." [Online]. Available: https://britishorigami.info/lister/german.php (Accessed: May 19, 2021).

[3] M. Giegher, *Li Tre Trattati*. Padua, Italy: Paolo Frambotto, 1639.

[4] J. Sallas, *Gefaltete Schönheit: Die Kunst Des Serviettenbrechens*. Freiburg I. Breisgau, Germany: Joan Sallas, 2010.

[5] "Tato folds." [Online]. Available: https://britishorigami.info/lister/tato_folds.php (Accessed: May 19, 2021).

[6] M. Miller and S. Martin, *Courtly Art of the Ancient Maya [published to Accompany the Exhibition Held at the National Gallery of Art, Washington, 4 April 2004-25 July 2004; Fine Arts Museums of San Francisco, California Palace of the Legion of Honor, 4 September 2004-2 January 2005]*. London, U.K.: Thames Hudson Ltd., 2004.

[7] J. Dambrogio *et al.*, "Unlocking history through automated virtual unfolding of sealed documents imaged by X-ray microtomography," *Nat. Commun.*, vol. 12, no. 1, pp. 1–10, 2021.

[8] K. Miura and M. Natori, "2-D array experiment on board a space flyer unit," *Space Solar Power Rev.*, vol. 5, no. 4, pp. 345–356, 1985.

[9] K. Miura *et al.*, "The science of Miura-ori: A review," in *Origami*, vol. 4. Bideford, U.K.: Kerswell Books, 2009, pp. 87–99.

[10] H. S. Rauschenbach, *Solar Cell Array Design Handbook: The Principles and Technology of Photovoltaic Energy Conversion*. Dordrecht, The Netherlands: Springer, 1980. [Online]. Available: https://doi.org/10.1007/978-94-011-7915-7

[11] R. A. Hyde, S. N. Dixit, A. H. Weisberg, and M. C. Rushford, "Eyeglass: A very large aperture diffractive space telescope," in *Proc. Highly Innovat. Space Telescope Concepts*, vol. 4849, 2002, pp. 28–39.

[12] D. Sigel, B. P. Trease, M. W. Thomson, D. R. Webb, P. Willis, and P. D. Lisman, "Application of origami in the starshade spacecraft blanket design," in *Proc. Int. Design Eng. Techn. Conf. Comput. Inf. Eng. Conf.*, 2014, p. 8.

[13] M. Arya *et al.*, "Origami-inspired optical shield for a starshade inner disk testbed: Design, fabrication, and analysis," in *Proc. AIAA Scitech Forum*, 2021, p. 0904.

[14] P. A. Warren, J. W. Steinbeck, R. J. Minelli, and C. Mueller, "Large, deployable S-band antenna for a 6U CubeSat," in *Proc. 31st Annu. AIAA/USU Conf. Small Satellites (SSC)*, 2015, pp. 1–7.

[15] N. Chahat, R. E. Hodges, J. Sauder, M. Thomson, E. Peral, and Y. Rahmat-Samii, "CubeSat deployable ka-band mesh reflector antenna development for earth science missions," *IEEE Trans. Antennas Propag.*, vol. 64, no. 6, pp. 2083–2093, Jun. 2016.

[16] P. K. Kelly, "A scalable deployable high gain antenna—DaHGR," in *Proc. 30th Annu AIAA/USU Conf. Small Satell.*, 2016, pp. 1–7.

[17] R. E. Hodges, D. J. Hoppe, M. J. Radway, and N. E. Chahat, "Novel deployable reflectarray antennas for CubeSat communications," in *IEEE MTT-S Int. Microw. Symp. Dig.*, Phoenix, AZ, USA, 2015, pp. 1–4.

[18] R. E. Hodges, N. Chahat, D. J. Hoppe, and J. D. Vacchione, "A deployable high-gain antenna bound for mars: Developing a new folded-panel reflectarray for the first CubeSat mission to mars," *IEEE Antennas Propag. Mag.*, vol. 59, no. 2, pp. 39–49, Apr. 2017.

[19] N. Chahat, G. Agnes, J. Sauder, and T. Cwik, "One meter deployable reflectarray antenna for earth science radars," in *Proc. IEEE Int. Symp. Antennas Propag. USNC/URSI Nat. Radio Sci. Meeting*, San Diego, CA, USA, 2017, pp. 245–246.

[20] M. Arya, J. F. Sauder, R. Hodges, and S. Pellegrino, "Large-area deployable reflectarray antenna for CubeSats," in *Proc. AIAA Scitech Forum*, 2019, p. 2257.

[21] R. Hodges *et al.*, "The ISARA mission—Flight demonstration of a high gain ka-band antenna for 100mbps telecom," in *Proc. 32nd Annu. AIAA/USU Conf. Small Satell.*, 2018, pp. 1–6.

[22] S. Gao, Y. Rahmat-Samii, R. E. Hodges, and X.-X. Yang, "Advanced antennas for small satellites," *Proc. IEEE*, vol. 106, no. 3, pp. 391–403, Mar. 2018.

[23] K. Miura and S. Pellegrino, *Forms and Concepts for Lightweight Structures*. New York, NY, USA: Cambridge Univ. Press, 2020.

[24] J. Morgan, S. P. Magleby, and L. L. Howell, "An approach to designing origami-adapted aerospace mechanisms," *J. Mech. Design*, vol. 138, no. 5, p. 10, 2016.

[25] K. C. Francis, L. T. Rupert, R. J. Lang, D. C. Morgan, S. P. Magleby, and L. L. Howell, "From crease pattern to product: Considerations to engineering origami-adapted designs," in *Proc. Int. Design Eng. Techn. Conf. Comput. Inf. Eng. Conf.*, 2014, p. 15.

[26] H. Hochfeld, "Process and machine for pleating pliable materials," U.S. Patent 2 901 951, 1959.

[27] H. M. Wingler, *The Bauhaus: Weimar, Dessau, Berlin, Chicago*, J. Stein, Ed. Cambridge, MA, USA: MIT Press, 1969 (Translated by W. Jabs and B. Gilbert).

[28] R. J. Lang, *Twists, Tilings, and Tessellations: Mathematical Methods for Geometric Origami*. Boca Raton, FL, USA: CRC Press, 2017.

[29] T. Tachi, "Generalization of rigid-foldable quadrilateral-mesh origami," *J. Int. Assoc. Shell Spatial Struct.*, vol. 50, no. 3, pp. 173–179, 2009.

[30] B. Kresling, "Folded tubes as compared to kikko ('tortoise-shell55) bamboo,"' in *Origami*, 3rd ed. New York, NY, USA: Barnes Noble, 2002, p. 197.

[31] K. Miura, *Proposition of Pseudo-Cylindrical Concave Polyhedral Shells*, Dept. Inst. Space Aeronaut. Sci., Univ. Tokyo, Tokyo, Japan, 1969.

[32] S. D. Guest and S. Pellegrino, "The folding of triangulated cylinders, part I: Geometric considerations," *J. Appl. Mech.*, vol. 61, no. 4, pp. 773–777, 1994.

[33] S. D. Guest and S. Pellegrino, "The folding of triangulated cylinders, part II: The folding process," *J. Appl. Mech.*, vol. 61, no. 4, pp. 778–783, 1994.

[34] S. D. Guest and S. Pellegrino, "The folding of triangulated cylinders, part III: Experiments," *J. Appl. Mech.*, vol. 63, no. 1, pp. 77–83, 1996.

[35] T. Fuse, *Spiral: Origami, Art, Design*. Freising, Germany: Viereck Verlag, 2012.

[36] J. Beynon, *Spring into Action, Bos Magazine*, vol. 142, Brit. Origami Soc., London, U.K., 1990.

[37] R. J. Lang, *Origami in Action: Paper Toys That Fly, Flag, Gobble and Inflate!*. New York, NY, USA: Macmillan, 1997.

[38] H. Scheel, "Space-saving storage of flexible sheets," U.S. Patent 3 848 821, Nov. 19, 1974.

[39] S. D. Guest and S. Pellegrino, "Inextensional wrapping of flat membranes," in *Proc. 1st Int. Seminar Struct. Morphol.*, vol. 25, 1992, pp. 203–215.

[40] S. A. Zirbel *et al.*, "Accommodating thickness in origami-based deployable arrays," *J. Mech. Design*, vol. 135, no. 11, p. 11, 2013.

[41] L. Dufour, L. S. Datashvili, F. Guinot, H. Legay, and G. Goussetis, "Origami deployable reflector antenna for CubeSats," in *Proc. AIAA Scitech Forum*, 2021, p. 1703.

[42] B. Liu *et al.*, "Topological kinematics of origami metamaterials," *Nat. Phys.*, vol. 14, no. 8, pp. 811–815, 2018.

[43] M. Arya, N. Lee, and S. Pellegrino, "Ultralight structures for space solar power satellites," in *Proc. 3rd AIAA Spacecraft Struct. Conf.*, 2016, p. 1950.

[44] M. Arya, "Packaging and deployment of large planar spacecraft structures," Ph.D. dissertation, Dept. Doctor Philos., California Inst. Technol., Pasadena, CA, USA, 2016.

[45] M. Arya, N. Lee, and S. Pellegrino, "Crease-free biaxial packaging of thick membranes with slipping folds," *Int. J. Solids Struct.*, vol. 108, pp. 24–39, Mar. 2017.

[46] T. Tachi, "Simulation of rigid origami," in *Origami*, vol. 4. Bideford, U.K.: Kerswell Books, 2009, pp. 175–187.

[47] R. D. Resch and H. Christiansen, "The design and analysis of kinematic folded plate systems," in *Proc. IASS Symp. Folded Plates Prismatic Struct.*, 1970.

[48] M. Schenk and S. D. Guest, "Origami folding: A structural engineering approach," in *Origami*, vol. 5. New York, NY, USA: Rosen Publ. Group, 2011, pp. 291–304.

[49] T. Tachi, "Rigid-foldable thick origami," in *Origami*, vol. 5. New York, NY, USA: Rosen Publ. Group, 2011, pp. 253–264.

[50] R. J. Lang, K. A. Tolman, E. B. Crampton, S. P. Magleby, and L. L. Howell, "A review of thickness-accommodation techniques in origami-inspired engineering," *Appl. Mech. Rev.*, vol. 70, no. 1, p. 20, 2018.

[51] E. A. P. Hernandez, D. J. Hartl, and D. C. Lagoudas, "Kinematics of origami structures with smooth folds," *J. Mech. Robot.*, vol. 8, no. 6, p. 22, 2016.

[52] D. A. Huffman, "Curvature and creases: A primer on paper," *IEEE Comput. Archit. Lett.*, vol. C-25, no. 10, pp. 1010–1019, Oct. 1976.

[53] J. P. Duncan and J. L. Duncan, "Folded developables," *Proc. Roy. Soc. London A, Math. Phys. Sci.*, vol. 383, no. 1784, pp. 191–205, 1982.

[54] D. Fuchs and S. Tabachnikov, "More on paperfolding," *Amer. Math. Monthly*, vol. 106, no. 1, pp. 27–35, 1999.

[55] E. D. Demaine, M. L. Demaine, D. A. Huffman, D. Koschitz, and T. Tachi, "Characterization of curved creases and rulings: Design and analysis of lens tessellations," in *Origami*, vol. 6. New York, NY, USA: Distrib. Infobase, 2015, pp. 209–230.

[56] E. D. Demaine, M. L. Demaine, D. A. Huffman, D. Koschitz, and T. Tachi, "Conic crease patterns with reflecting rule lines," in *Origami7: II. Mathematics*. St Albans, U.K.: Tarquin, 2018, pp. 573–589.

[57] E. T. Filipov, K. Liu, T. Tachi, M. Schenk, and G. H. Paulino, "Bar and hinge models for scalable analysis of origami," *Int. J. Solids Struct.*, vol. 124, pp. 26–45, Oct. 2017.

[58] T. Tachi. "Origamizer." [Online]. Available: https://tsg.ne.jp/TT/software/ (Accessed: Oct. 21, 2021).

[59] T. Tachi. "Freeform Origami." [Online]. Available: http://origami.c.u-tokyo.ac.jp/tachi/software/ (Accessed: Oct. 21, 2021).

[60] J. Mitani. "Ori-Revo: A Design Tool for 3D Origami of Revolution." [Online]. Available: http://mitani.cs.tsukuba.ac.jp/orirevo/ (Accessed: Oct. 21, 2021).

[61] R. J. Lang. "Tessellatica." 2015. [Online]. Available: https://langorigami.com/article/tessellatica/

[62] A. Ghassaei. "Origami Simulator." [Online]. Available: http://apps.amandaghassaei.com/OrigamiSimulator/ (Accessed: Oct. 21, 2021).

[63] E. Demaine. "Fold Spec, Viewer, API." [Online]. Available: https://github.com/edemaine/fold (Accessed: Oct. 21, 2021).

[64] K. Kuribayashi *et al.*, "Self-deployable origami stent grafts as a biomedical application of Ni-rich TiNi shape memory alloy foil," *Mater. Sci. Eng. A*, vol. 419, nos. 1–2, pp. 131–137, 2006.

[65] R. Fernandes and D. H. Gracias, "Self-folding polymeric containers for encapsulation and delivery of drugs," *Adv. Drug Del. Rev.*, vol. 64, no. 14, pp. 1579–1589, 2012.

[66] N. Bassik *et al.*, "Enzymatically triggered actuation of miniaturized tools," *J. Amer. Chem. Soc.*, vol. 132, no. 46, pp. 16314–16317, 2010.

[67] S. A. Zirbel, B. P. Trease, M. W. Thomson, R. J. Lang, S. P. Magleby, and L. H. Howell, "HanaFlex: A large solar array for space applications," in *Proc. Micro-and Nanotechnol. Sens. Syst. Appl. VII*, vol. 9467, 2015, Art. no. 94671C.

[68] M. Schenk, A. D. Viquerat, K. A. Seffen, and S. D. Guest, "Review of inflatable booms for deployable space structures: Packing and rigidization," *J. Spacecraft Rockets*, vol. 51, no. 3, pp. 762–778, 2014.

[69] L. Wilson, S. Pellegrino, and R. Danner, "Origami sunshield concepts for space telescopes," in *Proc. 54th AIAA/ASME/ASCE/AHS/ASC Struct. Struct. Dyn. Mater. Conf.*, 2013, p. 1594.

[70] B. Cheng, M. Kim, H. Lin, S. Fung, Z. Bush, and J. H. Seo, "Tessella: Interactive origami light," in *Proc. 6th Int. Conf. Tangible Embedded Embodied Interact.*, 2012, pp. 317–318.

[71] "Iain Sinclair Cardsharp 2 Credit Card Folding Safety Knife." Knife Center. [Online]. Available: http://www.knifecenter.com/item/ISCARDB2/iain-sinclair-cardsharp-credit-card-folding (Accessed: Oct. 21, 2021).

[72] H. F. Thorne, E. M. Wiegmann, M. J. Koes, and R. D. Daley, "Collapsible stroller," U.S. Patent A 29 343 043, May 18, 2010.

[73] S. Mintchev, L. Daler, G. L'Eplattenier, L. Saint-Raymond, and D. Floreano, "Foldable and self-deployable pocket sized quadrotor," in *Proc. IEEE Int. Conf. Robot. Autom. (ICRA)*, Seattle, WA, USA, 2015, pp. 2190–2195.

[74] H. Shigemune, S. Maeda, Y. Hara, N. Hosoya, and S. Hashimoto, "Origami robot: A self-folding paper robot with an electrothermal actuator created by printing," *IEEE/ASME Trans. Mechatronics*, vol. 21, no. 6, pp. 2746–2754, Dec. 2016.

[75] C. H. Belke and J. Paik, "Mori: A modular origami robot," *IEEE/ASME Trans. Mechatronics*, vol. 22, no. 5, pp. 2153–2164, Oct. 2017.

[76] Y. Li, W. Liu, Y. Deng, W. Hong, and H. Yu, "Miura-ori enabled stretchable circuit boards," *NPJ Flexible Electron.*, vol. 5, no. 1, pp. 1–9, 2021.

[77] X. Xiang, W. Qiang, B. Hou, P. Tran, and G. Lu, "Quasi-static and dynamic mechanical properties of Miura-ori metamaterials," *Thin Walled Struct.*, vol. 157, Dec. 2020, Art. no. 106993.

[78] Y. Hou, Y. Wang, M. Yu, Z. Wang, and H. Yu, "Miura-ori metastructure enhanced conductive elastomers," *Adv. Mater. Technol.*, vol. 5, no. 8, 2020, Art. no. 2000249.

[79] M. Yu, W. Yang, Y. Yu, X. Cheng, and Z. Jiao, "A crawling soft robot driven by pneumatic foldable actuators based on Miura-ori," *Actuators*, vol. 9, no. 2, p. 26, 2020.

[80] J. Cai, M. Li, Y. Li, Y. Ding, and J. Feng, "Deployment simulation of a scalable planar gossamer space structure based on Miura-ori pattern," *Adv. Space Res.*, vol. 67, no. 10, pp. 3343–3353, 2021.

[81] B. Liu and Y. Sun, "Free vibration analysis of carbon-fiber-reinforced Miura-ori core sandwich beam: Theoretical prediction and numerical simulation," *Mech. Adv. Mater. Struct.*, pp. 1–10, Sep. 2020.

[82] C. Yuan *et al.*, "3D printed reversible shape changing soft actuators assisted by liquid crystal elastomers," *Soft Matter*, vol. 13, no. 33, pp. 5558–5568, 2017.

[83] X. Zhang, M. Yu, W. Yang, Y. Yu, Y. Ding, and Z. Jiao, "A flexible mechanical arm based on Miura-ori," in *Proc. Int. Conf. Intell. Robot. Appl.*, 2020, pp. 538–544.

[84] M. Islam, J. Flach, and R. Martinez-Duarte, "Carbon origami: A method to fabricate lightweight carbon cellular materials," *Carbon*, vol. 133, pp. 140–149, Jul. 2018.

[85] H. Banerjee, N. Pusalkar, and H. Ren, "Preliminary design and performance test of tendon-driven origami-inspired soft peristaltic robot," in *Proc. IEEE Int. Conf. Robot. Biomimetics (ROBIO)*, Kuala Lumpur, Malaysia, 2018, pp. 1214–1219.

[86] K. Westra, F. Dunne, S. Kulsa, M. Hunt, and J. Leachman, "Compliant polymer origami bellows in cryogenics," *Cryogenics*, vol. 114, Mar. 2021, Art. no. 103226.

[87] M. Norman and K. Arjomandi, "Origami applications in structural engineering: A look at temporary shelters," in *Proc. 2nd World Congr. Civil Struct. Environ. Eng. (CSEE)*, vol. 130, 2017, pp. 2371–2452.

[88] H. Feng, J. Ma, Y. Chen, and Z. You, "Twist of tubular mechanical metamaterials based on waterbomb origami," *Sci. Rep.*, vol. 8, no. 1, pp. 1–13, 2018.

[89] S. Sadeghi and S. Li, "Dynamic folding of origami by exploiting asymmetric bi-stability," *Extreme Mech. Lett.*, vol. 40, Oct. 2020, Art. no. 100958.

[90] E. Rivas-Adrover, "Origami-scissor hinged geometry method," in *Proc. 7th Int. Meeting Origami Sci. Math. Educ.*, 2018, pp. 1–12.

[91] Z. Meng, W. Chen, T. Mei, Y. Lai, Y. Li, and C. Q. Chen, "Bistability-based foldable origami mechanical logic gates," *Extreme Mech. Lett.*, vol. 43, Feb. 2021, Art. no. 101180.

[92] H. Feng, R. Peng, J. Ma, and Y. Chen, "Rigid foldability of generalized triangle twist origami pattern and its derived 6R linkages," *J. Mech. Robot.*, vol. 10, no. 5, p. 13, 2018.

[93] H. Feng, R. Peng, S. Zang, J. Ma, and Y. Chen, "Rigid foldability and mountain-valley crease assignments of square-twist origami pattern," *Mech. Mach. Theory*, vol. 152, Oct. 2020, Art. no. 103947.

[94] T. A. Evans, R. J. Lang, S. P. Magleby, and L. L. Howell, "Rigidly foldable origami twists," in *Origami*, vol. 6. New York, NY, USA: Distrib. Infobase, 2015, pp. 119–130.

[95] B. P. DeFigueiredo, N. A. Pehrson, K. A. Tolman, E. Crampton, S. P. Magleby, and L. L. Howell, "Origami-based design of conceal-and-reveal systems," *J. Mech. Robot.*, vol. 11, no. 2, p. 9, 2019.

[96] S. Lee, S. I. H. Shah, H. L. Lee, and S. Lim, "Frequency-reconfigurable antenna inspired by origami flasher," *IEEE Antennas Wireless Propag. Lett.*, vol. 18, pp. 1691–1695, 2019.

[97] N. A. Pehrson, D. C. Ames, S. P. Smith, S. P. Magleby, and M. Arya, "Self-deployable, self-stiffening, and retractable origami-based arrays for spacecraft," *AIAA J.*, vol. 58, no. 7, pp. 3221–3228, 2020.

[98] V. Srinivas and R. L. Harne, "Directing acoustic energy by flasher-based origami inspired arrays," *J. Acoust. Soc. Amer.*, vol. 148, no. 5, pp. 2935–2944, 2020.

[99] C. Guang and Y. Yang, "An approach to designing deployable mechanisms based on rigid modified origami flashers," *J. Mech. Design*, vol. 140, no. 8, p. 11, 2018.

[100] K. Miura, "Map fold a la Miura style, its physical characteristics and application to the space science," in *Research Pattern Formation*. Tokyo, Japan: KTK Sci. Publ., 1994, pp. 77–90.

[101] N. Turner, B. Goodwine, and M. Sen, "A review of origami applications in mechanical engineering," *Proc. Inst. Mech. Eng. C, J. Mech. Eng. Sci.*, vol. 230, no. 14, pp. 2345–2362, 2016.

[102] Y. Yoshimura, "On the mechanism of buckling of a circular cylindrical shell under axial compression," UNT Libraries Govt. Documents Dept., University of North Texas Libraries, UNT Digital Library, Denton, TX, USA, Rep. NACA-TM-1390, Jul. 1955. Accessed: Oct. 21, 2021. [Online]. Available: https://digital.library.unt.edu/ark:/67531/metadc62872/

[103] L. Paez, G. Agarwal, and J. Paik, "Design and analysis of a soft pneumatic actuator with origami shell reinforcement," *Soft Robot.*, vol. 3, no. 3, pp. 109–119, 2016.

[104] K. Yang, S. Xu, J. Shen, S. Zhou, and Y. M. Xie, "Energy absorption of thin-walled tubes with pre-folded origami patterns: Numerical simulation and experimental verification," *Thin-Walled Struct.*, vol. 103, pp. 33–44, Jun. 2016.

[105] J. Cai, X. Deng, Y. Xu, and J. Feng, "Motion analysis of a foldable barrel vault based on regular and irregular Yoshimura Origami," *J. Mech. Robot.*, vol. 8, no. 2, 2016, Art. no. 021017.

[106] Y. Chen, H. Feng, J. Ma, R. Peng, and Z. You, "Symmetric waterbomb origami," *Proc. Royal Soc. A Math. Phys. Eng. Sci.*, vol. 472, no. 2190, 2016, Art. no. 20150846.

[107] B. H. Hanna, J. M. Lund, R. J. Lang, S. P. Magleby, and L. L. Howell, "Waterbomb base: A symmetric single-vertex bistable origami mechanism," *Smart Mater. Struct.*, vol. 23, no. 9, 2014, Art. no. 094009.

[108] C. D. Onal, R. J. Wood, and D. Rus, "An origami-inspired approach to worm robots," *IEEE/ASME Trans. Mechatronics*, vol. 18, no. 2, pp. 430–438, Apr. 2013.

[109] D.-Y. Lee, J.-S. Kim, S.-R. Kim, J.-S. Koh, and K.-J. Cho, "The deformable wheel robot using magic-ball origami structure," in *Proc. Int. Design Eng. Tech. Conf. Comput. Inf. Eng. Conf.*, 2013, p. 9.

[110] T. Tachi and T. C. Hull, "Self-foldability of rigid origami," *J. Mech. Robot.*, vol. 9, no. 2, 2017, Art. no. 021008.

[111] E. Morris, D. A. McAdams, and R. Malak, "The state of the art of origami-inspired products: A review," in *Proc. ASME Int. Design Eng. Tech. Conf. Comput. Inf. Eng. Conf.*, Charlotte, NC, USA, Aug. 2016, Art. no. V05BT07A014. [Online]. Available: https://doi.org/10.1115/DETC2016-59629

[112] M. Meloni *et al.*, "Engineering origami: A comprehensive review of recent applications, design methods, and tools," *Adv. Sci.*, vol. 8, no. 13, 2021, Art. no. 2000636.

[113] Y. Chen, J. Yan, and J. Feng, "Geometric and kinematic analyses and novel characteristics of origami-inspired structures," *Symmetry*, vol. 11, no. 9, p. 1101, 2019.

[114] D. Bolanos *et al.*, "Considering thickness-accommodation, nesting, grounding and deployment in design of Miura-ori based space arrays," in *Proc. 5th ASME/IFToMM Int. Conf. Reconfigurable Mech. Robots*, 2021.

[115] D. W. Andrews, S. P. Magleby, and L. L. Howell, "Thickness-utilizing deployable hard stops for origami-based design applications," *Mech. Sci.*, vol. 11, no. 2, pp. 395–410, 2020.

[116] J. Butler, N. Pehrson, and S. Magleby, "Folding of thick origami through regionally sandwiched compliant sheets," *J. Mech. Robot.*, vol. 12, no. 1, 2020, Art. no. 011019.

[117] A. Firouzeh and J. Paik, "An under-actuated origami gripper with adjustable stiffness joints for multiple grasp modes," *Smart Mater. Struct.*, vol. 26, no. 5, 2017, Art. no. 055035.

[118] P. D. Shemenski and B. P. Trease, "Compact directional and frictional hinges for flat folding applications," in *Proc. ASME Int. Design Eng. Tech. Conf. Comput. Inf. Eng. Conf.*, Quebec City, QC, Canada, Aug. 2018, Art. no. V05BT07A064. [Online]. Available: https://doi.org/10.1115/DETC2018-86225

[119] G. Horner and M. Elliott, "A fabrication and deployment approach for a Miura-ori solar sail model," in *Proc. 43rd AIAA/ASME/ASCE/AHS/ASC Struct. Struct. Dyn. Mater. Conf.*, 2002, p. 1708.

[120] B. Cowan and P. R. Von Lockette, "Fabrication, characterization, and heuristic trade space exploration of magnetically actuated Miura-ori origami structures," *Smart Mater. Struct.*, vol. 26, no. 4, 2017, Art. no. 045015.

[121] S. Yao, S. V. Georgakopoulos, B. Cook, and T. M., "A novel reconfigurable origami accordion antenna," in *Proc. IEEE MTT-S Int. Microw. Symp. (IMS)*, 2014, pp. 1–4.

[122] M. Hamza, C. L. Zekios, and S. V. Georgakopoulos, "A thick origami reconfigurable and packable patch array with enhanced beam steering," *IEEE Trans. Antennas Propag.*, vol. 68, no. 5, pp. 3653–3663, May 2020.

[123] A. Biswas, C. L. Zekios, and S. V. Georgakopoulos, "Transforming single-band static FSS to dual-band dynamic FSS using origami," *Sci. Rep.*, vol. 10, no. 1, pp. 1–12, 2020.

[124] D. H. Le and S. Lim, "Four-mode programmable metamaterial using ternary foldable origami," *ACS Appl. Mater. Interfaces*, vol. 11, no. 31, pp. 28554–28561, 2019.

[125] C. C. H. Ng and P. R. Young, "Origami folding technique using flexible substrate with arrays of Vivaldi antennas," in *Proc. Eur. Conf. Antennas Propag.*, Jan. 2018, p. 4.

[126] P. M. Njogu *et al.*, "Evaluation of planar inkjet-printed antennas on a low-cost origami flapping robot," *IEEE Access*, vol. 8, pp. 164103–164113, 2020.

[127] K. Fuchi, A. R. Diaz, E. J. Rothwell, R. O. Ouedraogo, and J. Tang, "An origami tunable metamaterial," *J. Appl. Phys.*, vol. 111, no. 8, 2012, Art. no. 084905.

[128] K. Fuchi, J. Tang, B. Crowgey, A. R. Diaz, E. J. Rothwell, and R. O. Ouedraogo, "Origami tunable frequency selective surfaces," *IEEE Antennas Wireless Propag. Lett.*, vol. 11, pp. 473–475, 2012.

[129] K. Fuchi *et al.*, "Spatial tuning of a RF frequency selective surface through origami," in *Proc. XXVI Autom. Target Recognit.*, vol. 9844, 2016, Art. no. 98440W.

[130] D. Sessions *et al.*, "Investigation of fold-dependent behavior in an origami-inspired FSS under normal incidence," *Progr. Electromagn. Res. M*, vol. 63, pp. 131–139, Jan. 2018.

[131] D. Sessions, A. Cook, K. Fuchi, A. Gillman, G. Huff, and P. Buskohl, "Origami-inspired frequency selective surface with fixed frequency response under folding," *Sensors*, vol. 19, no. 21, p. 4808, 2019.

[132] D. M. Sessions *et al.*, "Folding, tessellation, and deployment of an origami-inspired active-material-enabled self-folding reflector antenna," in *Proc. IEEE Int. Symp. Antennas Propag. USNC/URSI Nat. Radio Sci. Meeting*, 2018, pp. 929–930.

[133] J. Kimionis, M. Isakov, B. S. Koh, A. Georgiadis, and M. M. Tentzeris, "3D-printed origami packaging with inkjet-printed antennas for RF harvesting sensors," *IEEE Trans. Microw. Theory Techn.*, vol. 63, no. 12, pp. 4521–4532, Dec. 2015.

[134] G. J. Hayes, Y. Liu, J. Genzer, G. Lazzi, and M. D. Dickey, "Self-folding origami microstrip antennas," *IEEE Trans. Antennas Propag.*, vol. 62, no. 10, pp. 5416–5419, Oct. 2014.

[135] S. Jape *et al.*, "Self-foldable origami reflector antenna enabled by shape memory polymer actuation," *Smart Mater. Struct.*, vol. 29, no. 11, 2020, Art. no. 115011.

[136] S. A. Nauroze, L. S. Novelino, M. M. Tentzeris, and G. H. Paulino, "Continuous-range tunable multilayer frequency-selective surfaces using origami and inkjet printing," *Proc. Nat. Acad. Sci.*, vol. 115, no. 52, pp. 13210–13215, 2018.

[137] S. A. Nauroze and M. M. Tentzeris, "A thermally actuated fully inkjet-printed origami-inspired multilayer frequency selective surface with continuous-range tunability using polyester-based substrates," *IEEE Trans. Microw. Theory Techn.*, vol. 67, no. 12, pp. 4944–4954, Dec. 2019.

[138] Y. Xu, Y. Kim, M. M. Tentzeris, and S. Lim, "Bi-directional loop antenna array using magic cube origami," *Sensors*, vol. 19, no. 18, p. 3911, 2019.

[139] W. Su, R. Bahr, S. A. Nauroze, and M. M. Tentzeris, "3D printed reconfigurable helical antenna based on microfluidics and liquid metal alloy," in *Proc. IEEE Int. Symp. Antennas Propag. (APSURSI)*, 2016, pp. 469–470.

[140] W. Su, S. A. Nauroze, B. Ryan, and M. M. Tentzeris, "Novel 3D printed liquid-metal-alloy microfluidics-based zigzag and helical antennas for origami reconfigurable antenna 'trees,'" in *Proc. IEEE MTT-S Int. Microw. Symp. (IMS)*, 2017, pp. 1579–1582.

[141] W. Su, R. Bahr, S. A. Nauroze, and M. M. Tentzeris, "Novel 3D-printed 'Chinese fan' bow-tie antennas for origami/shape-changing configurations," in *Proc. IEEE Int. Symp. Antennas Propag. USNC/URSI Nat. Radio Sci. Meeting*, 2017, pp. 1245–1246.

[142] S. I. H. Shah, M. M. Tentzeris, and S. Lim, "Low-cost circularly polarized origami antenna," *IEEE Antennas Wireless Propag. Lett.*, vol. 16, pp. 2026–2029, 2017.

[143] S. I. H. Shah, M. M. Tentzeris, and S. Lim, "A deployable quasi-Yagi monopole antenna using three origami magic spiral cubes," *IEEE Antennas Wireless Propag. Lett.*, vol. 18, pp. 147–151, 2019.

[144] S. R. Seiler *et al.*, "Physical reconfiguration of an origami-inspired deployable microstrip patch antenna array," in *Proc. IEEE Int. Symp. Antennas Propag. USNC/URSI Nat. Radio Sci. Meeting*, 2017, pp. 2359–2360.

[145] J. Costantine *et al.*, "UHF deployable helical antennas for CubeSats," *IEEE Trans. Antennas Propag.*, vol. 64, no. 9, pp. 3752–3759, Sep. 2016.

[146] N. Miguélez-Gómez *et al.*, "Thickness-accommodation in X-band origami-based reflectarray antenna for small satellites applications," in *Proc. IEEE Int. Conf. Wireless Space Extreme Environ. (WiSEE)*, 2020, pp. 54–59.

[147] Y. Cui, A. Eid, and M. M. Tentzeris, "A 3D-printed mm-Wave deployable origami dielectric reflectarray antenna," in *Proc. IEEE Int. Symp. Antennas Propag. North Amer. Radio Sci. Meeting*, 2020, pp. 1679–1680.

[148] S. I. H. Shah and S. Lim, "Bioinspired DNA origami quasi-Yagi helical antenna with beam direction and beamwidth switching capability," *Sci. Rep.*, vol. 9, Oct. 2019, Art. no. 14312.

[149] M. Hwang, G. Kim, S. Kim, and N. S. Jeong, "Origami-inspired radiation pattern and shape reconfigurable dipole array antenna at C-band for CubeSat applications," *IEEE Trans. Antennas Propag.*, vol. 69, no. 5, pp. 2697–2705, May 2021.

[150] F. A. Espinal *et al.*, "Circularly-polarised origami-inspired folding patch antenna sub-array," *IET Microw. Antennas Propag.*, vol. 14, no. 11, pp. 1262–1271, 2020.

[151] S. B. Venkatakrishnan, A. Johnson, M. W. Nichols, J. A. C. Troccola, and J. L. Volakis, "Dynamically reconfigurable and packable multifunctional origami antennas and arrays," in *Proc. Int. Workshop Antenna Technol. (iWAT)*, 2020, pp. 1–2.

[152] S. Alharbi *et al.*, "E-textile origami dipole antennas with graded embroidery for adaptive RF performance," *IEEE Antennas Wireless Propag. Lett.*, vol. 17, pp. 2218–2222, 2018.

[153] X. Liu, S. Yao, B. S. Cook, M. M. Tentzeris, and S. V. Georgakopoulos, "An origami reconfigurable axial-mode bifilar helical antenna," *IEEE Trans. Antennas Propag.*, vol. 63, no. 12, pp. 5897–5903, Dec. 2015.

[154] X. Liu, S. V. Georgakopoulos, and S. Rao, "A design of an origami reconfigurable QHA with a foldable reflector [antenna applications corner]," *IEEE Antennas Propag. Mag.*, vol. 59, no. 4, pp. 78–105, Aug. 2017.

[155] S. Yao, X. Liu, J. Gibson, and S. V. Georgakopoulos, "Deployable origami Yagi loop antenna," in *Proc. IEEE Int. Symp. Antennas Propag. USNC/URSI Nat. Radio Sci. Meeting*, 2015, pp. 2215–2216.

[156] X. Liu, C. L. Zekios, and S. V. Georgakopoulos, "Analysis of a packable and tunable origami multi-radii helical antenna," *IEEE Access*, vol. 7, pp. 13003–13014, 2019.

[157] C. L. Zekios *et al.*, "Electromagnetic and mechanical analysis of an origami helical antenna encapsulated by fabric," in *Proc. ASME Int. Design Eng. Tech. Conf. Comput. Inf. Eng. Conf.*, 2019, p. 5.

[158] S. Yao, Y. Bonan, Y. Shafiq, and S. V. Georgakopoulos, "Rigid origami based reconfigurable conical spiral antenna," in *Proc. IEEE Int. Symp. Antennas Propag. USNC/URSI Nat. Radio Sci. Meeting*, 2018, pp. 179–180.

[159] J. O. Jacobsen, G. Chen, L. L. Howell, and S. P. Magleby, "Lamina emergent torsional (LET) joint," *Mech. Mach. Theory*, vol. 44, no. 11, pp. 2098–2109, 2009.

[160] A.-S. Kaddour *et al.*, "A foldable and reconfigurable monolithic reflectarray for space applications," *IEEE Access*, vol. 8, pp. 219355–219366, 2020.

[161] A. J. Rubio *et al.*, "An origami-inspired foldable reflectarray on a straight-major square-twist pattern," in *Proc. IEEE 21st Wireless Microw. Techinol. Conf. (WAMICON)*, 2021, pp. 1–4.

[162] K. A. Tolman, R. J. Lang, S. P. Magleby, and L. L. Howell, "Split-vertex technique for thickness-accommodation in origami-based mechanisms," in *Proc. Int. Design Eng. Tech. Conf. Comput. Inf. Eng. Conf.*, 2017, p. 10.

[163] A.-S. Kaddour, C. L. Zekios, and S. V. Georgakapoulos, "A reconfigurable origami reflectarray," in *Proc. 14th Eur. Conf. Antennas Propag. (EuCAP)*, 2020, pp. 1–4.

[164] A. J. Rubio, A.-S. Kaddour, S. V. Georgakopoulos, C. Ynchausti, S. Magleby, and L. L. Howell, "A deployable hexagonal reflectarray antenna for space applications," in *Proc. United States Nat. Committee URSI Nat. Radio Sci. Meeting (USNC-URSI NRSM)*, 2021, pp. 136–137.

[165] C. A. Velez *et al.*, "Reconfigurable and deployable Miura-ori RA analysis for satellite applications," in *Proc. IEEE 21st Annu. Wireless Microw. Technol. Conf. (WAMICON)*, 2021, pp. 1–3.

[166] A.-S. Kaddour, C. L. Zekios, and S. Georgakopoulos, "Reconfigurable arrays with multiple unit cells," U.S. Patent 10 931 022, Feb. 23, 2021.

[167] R. J. Lang. "Treemaker." [Online]. Available: https://langorigami.com/article/treemaker/ (Accessed: Oct. 21, 2021).

[168] J. Mitani. "Oripa: Origami Pattern Editor." [Online]. Available: http://mitani.cs.tsukuba.ac.jp/oripa/ (Accessed: Oct. 21, 2021).

[169] A. Bateman. "Tess: Origami Tessellation Software." [Online]. Available: http://www.papermosaics.co.uk/software.html (Accessed: Oct. 21, 2021).

[170] M. R. Khan, C. L. Zekios, S. Georgakopoulos, and S. Bhardwaj, "Automated design and optimization of origami electromagnetic structures [em programmer's notebook]," *IEEE Antennas Propag. Mag.*, vol. 63, no. 2, pp. 89–102, Apr. 2021.

[171] J. D. Kraus, "Helical beam antenna," *Electronics*, vol. 20, no. 4, pp. 109–111, 1947.

[172] H. Wheeler, "A helical antenna for circular polarization," *Proc. IRE*, vol. 35, no. 12, pp. 1484–1488, Dec. 1947.

[173] A. Adams, R. Greenough, R. Wallenberg, A. Mendelovicz, and C. Lumjiak, "The quadrifilar helix antenna," *IEEE Trans. Antennas Propag.*, vol. 22, no. 2, pp. 173–178, Mar. 1974.

[174] C. Jianguo, D. Xiaowei, Z. Ya, F. Jian, and T. Yongming, "Bistable behavior of the cylindrical origami structure with Kresling pattern," *J. Mech. Design*, vol. 137, no. 6, p. 8, 2015.

[175] S. V. Georgakopoulos and X. Liu, "Deployable and reconfigurable origami antennas using fabric, textile or other material encapsulation and/or scaffolding," U.S. Patent 10 347 962, Jul. 9, 2019.

[176] "Elektrisola." [Online]. Available: www.elektrisola.com (Accessed: Oct. 21, 2021).

STAVROS V. GEORGAKOPOULOS (Senior Member, IEEE) received the Diploma degree in electrical engineering from the University of Patras, Patras, Greece, in June 1996, and the M.S. degree in electrical engineering and the Ph.D. degree in electrical engineering from Arizona State University, Tempe, AZ, USA, in 1998 and 2001, respectively. From 2001 to 2007, he was the Principal Engineer with SV Microwave, Inc. Since 2007, he has been with the Department of Electrical and Computer Engineering, Florida International University, Miami, FL, USA, where he is currently a Professor and the Director of the Transforming Antennas Center (a research center on foldable/origami, physically reconfigurable, and deployable antennas) and the RF Communications, Millimeter-Waves, and Terahertz Lab. His current research interests relate to novel antennas, arrays, RFID, microwave and RF systems, novel sensors and wireless powering of portable, as well as wearable and implantable devices. He received the 2015 FIU President's Council Worlds Ahead Faculty Award, which is the highest honor FIU extends to a faculty member for excelling in research, teaching, mentorship, and service. He served as an Associate Editor for the IEEE TRANSACTIONS ON ANTENNAS AND PROPAGATION from 2013 to 2019. He has been an Associate Editor of the IEEE OPEN JOURNAL OF ANTENNAS AND PROPAGATION since 2019.

CONSTANTINOS L. ZEKIOS (Member, IEEE) received the Diploma degree (Hons.) in electrical and computer engineering, the M.S. degree (Hons.) in electrical and computer engineering communication and satellite telecommunication systems, and the Ph.D. degree (Hons.) in electrical and computer engineering from the Democritus University of Thrace, Xanthi, Greece, in 2008, 2011, and 2015, respectively. From January 2016 to May 2018, he was a Postdoctoral Researcher with the Electrical and Computer Engineering Department, University of Massachusetts Amherst, MA, USA, and from May 2018 to August 2020, he was a Postdoctoral Research Fellow with the Transforming Antennas Center, Florida International University, Miami, FL, USA, where he is currently a Research Assistant Professor with the Department of Electrical and Computer Engineering. His main research interests include computational electromagnetics, optimization methods, photonics, antennas, antenna arrays, electromagnetic surfaces, beamforming networks, and microwave engineering.

ABDUL SATTAR-KADDOUR (Member, IEEE) received the B.S. degree in electronics from the Faculty of Science, Lebanese University, Lebanon, in 2011, the B.S. and M.S. degrees in electronics and embedded systems engineering from the Grenoble Institute of Technology, Grenoble, France, in 2012 and 2014, respectively, and the Ph.D. degree in optics and radiofrequency from the Grenoble Alpes University, Grenoble, in 2018. His Ph.D. has been realized at CEA-LETI, Grenoble, where he developed electrically small and frequency reconfigurable antennas for space applications. In 2018, he joined the Xlim Research Institute, Limoges, France. Since 2019, he has been a Research Fellow with the Transforming Antennas Center, Florida International University, Miami, FL, USA. He has four issued patents in the U.S. Patent Office. His main research interests include electrically small antennas, reconfigurable antennas, antenna arrays, reflectarrays, and wireless power transfer systems. He serves as a reviewer for the numerous IEEE journals in the field of microwave, antennas, and propagation.

MUHAMMAD HAMZA (Graduate Student Member, IEEE) received the B.S. degree in electrical engineering from Syed Babar Ali School of Science and Engineering (SBASSE), Lahore University of Management Sciences (LUMS), Lahore, Pakistan, in 2017. He is currently pursuing the Ph.D. degree with the Transforming Antennas Center, Florida International University, under Dr. Georgakopoulos. He worked as a Research Assistant with the field of antenna design with SBASSE, LUMS, from 2017 to 2018. His main research interests include reconfigurable antennas and ultra-wideband antenna arrays.

AKASH BISWAS (Graduate Student Member, IEEE) was born in Chittagong, Bangladesh. He received the B.S. degree in electrical and electronic engineering from American International University–Bangladesh (AIUB) in 2016. He is currently pursuing the Ph.D. degree with Florida International University, where he is a Research Assistant with Transforming Antennas Center. He was a Lecturer with the Department of Electrical and Electronic Engineering, Port City International University, Chittagong, for one and half years. His main research interest includes frequency selective surface, microwave absorbers, and metasurface antennas. He is the recipient of the Best Student Paper Award in WAMICON 2021.

BROOKLYN CLARK is currently pursuing the B.S. degree in mechanical engineering. She is a Research Assistant with the Compliant Mechanism Research Group, Brigham Young University. Her research is focused on deployable origami arrays.

COLLIN YNCHAUSTI received the B.S. degree in mechanical engineering from the University of Utah, Salt Lake City, UT, USA, in 2015. He is currently pursuing the Ph.D. degree in mechanical engineering with Brigham Young University (BYU), Provo, UT, USA, 84602. Prior to BYU, he was a Product Line Engineer with Bechtel Marine Propulsion Corporation. He is currently a Research Assistant with the Compliant Mechanism Research Group, BYU, researching compliant mechanisms and deployable systems.

LARRY L. HOWELL received the B.S. degree from Brigham Young University (BYU) and the M.S. and Ph.D. degrees from Purdue University. Prior to joining BYU, he was with Engineering Methods and an Engineer on the YF-22 (the prototype for the U.S. Air Force F-22 Raptor). He is the Co-Editor of the *Handbook of Compliant Mechanisms* and has authored *Compliant Mechanisms*, which are published in English and Chinese. His lab's work has also been reported in popular venues, such as *Newsweek*, *Scientific American*, *The Economist*, *Smithsonian Magazine*, and the PBS documentary program *NOVA*. His research focuses on compliant mechanisms, including origami-inspired mechanisms, space mechanisms, and medical devices. He is the recipient of the ASME Machine Design Award, the ASME Mechanisms & Robotics Award, the Theodore von Kármán Fellowship, the NSF Career Award, the Purdue Outstanding Mechanical Engineer (Alumni Award), and the BYU Karl G. Maeser Distinguished Lecturer Award (BYU's Highest Faculty Award). He is a Fellow of ASME.

SPENCER P. MAGLEBY received the B.S. and M.S. degrees in civil engineering from Brigham Young University (BYU) and the Ph.D. degree in mechanical engineering from the University of Wisconsin–Madison. He is a Professor of Mechanical Engineering with BYU, where he is currently the Honors Program Director. He spent six years in the military aircraft industry developing tools for advanced aircraft design and manufacture. He teaches design at the graduate and undergraduate level. At BYU, he has pursued research in areas of product design, technology development and engineering education and has been especially active in developing new technologies and applications related to compliant mechanisms and the use of origami to inspire innovative product design. He is an avid road cyclist, amateur architect, and design junkie.

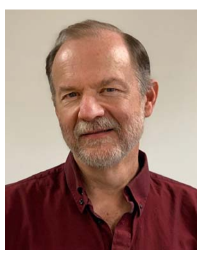

ROBERT J. LANG (Member, IEEE) received the B.S. degree in electrical engineering from the California Institute of Technology (Caltech), the M.S. degree in electrical engineering from Stanford University, and the Ph.D. degree in applied physics from Caltech. After 15 years in the lasers and optoelectronics field with stints with NASA/JPL and Spectra Diode Laboratories, he became a full-time Origami Artist and a Consultant. He continues to work in both the art and science of Origami. He has authored or coauthored over 50 patents and over 100 technical papers in optoelectronics and the mathematics and technology of folding. He was an Associate Editor of the IEEE JOURNAL OF QUANTUM ELECTRONICS from 1996 to 2001 and from 2004 to 2007, and the Editor-in-Chief from 2007 to 2010. He is a Fellow of the Optical Society of America and the American Mathematical Society, and is a Distinguished Alumnus of Caltech.